IMPACTS OF OLANZAPINE COUPLED WITH OR WITHOUT METFORMIN ADMINISTRATION ON THE EXPRESSION OF CANNABINOID AND MELANOCORTIN RECEPTORS IN RATS

A THESIS SUBMITTED TO
THE GRADUATE SCHOOL OF NATURAL AND APPLIED SCIENCES OF
MIDDLE EAST TECHNICAL UNIVERSITY

BY

ADITYA KEMAL JACOB ALIS

IN PARTIAL FULFILLMENT OF THE REQUIREMENTS
FOR
THE DEGREE OF MASTER OF SCIENCE
IN
BIOCHEMISTRY

AUGUST 2017

Approval of the thesis:

IMPACTS OF OLANZAPINE COUPLED WITH OR WITHOUT METFORMIN ADMINISTRATION ON THE EXPRESSION OF CANNABINOID AND MELANOCORTIN RECEPTORS IN RATS

Submitted by **ADITYA KEMAL JACOB ALIS** in partial fulfillment of the requirements for the degree of **Master of Science in Biochemistry Department, Middle East Technical University** by,

Prof. Dr. Gülbin Dural Ünver
Dean, **Graduate School of Natural and Applied Sciences, METU** _____

Prof. Dr. Bülent İçgen
Head of Department, **Biochemistry Dept., METU**

Assoc. Prof. Dr. Tülin Yanık
Supervisor, **Biological Sciences Dept., METU**

Examining Committee Members:

Prof. Dr. Semra Kocabıyık
Biological Sciences Dept., METU

Assoc. Prof. Dr. Tülin Yanık
Biological Sciences Dept., METU

Assoc. Prof. Dr. Çağdaş D. Son
Biological Sciences Dept., METU

Prof. Dr. Fatih İzgü
Biological Sciences Dept., METU

Assist. Prof. Dr. Süheyla Doğan Bulut
Dışkapı Yıldırım Beyazıt Eğitim Ve Araştırma Hastanesi

Date: 05.07.2017

I hereby declare that all information in this document has been obtained and presented in accordance with academic rules and ethical conduct. I also declare that, as required by these rules and conduct, I have fully cited and referenced all material and results that are not original to this work.

Name, Last name: ADITYA KEMAL

JACOB ALIS

Signature:

ABSTRACT

IMPACTS OF OLANZAPINE COUPLED WITH OR WITHOUT METFORMIN ADMINISTRATION ON THE EXPRESSION OF CANNABINOID AND MELANOCORTIN RECEPTORS IN RATS

Jacob Alis, Aditya Kemal

M.Sc, Biochemistry, Department of Biochemistry

Supervisor: Assoc. Prof. Dr. Tülin Yanık

August 2017, 94 pages

Secondary generation antipsychotics (SGA) were lauded as an improvement over first generation antipsychotics (FGA) in terms of both efficacies and reduced metabolic side effects such as obesity and diabetic phenotypes (1). However, SGAs were still plagued by a plethora of aforementioned metabolic side effects, albeit at reduced severity compared to the FGAs. While the side effects of SGAs had been extensively investigated through different experiments, the exact mechanism of the SGAs on the metabolic disorders' development had not been determined. In our experiment the impacts of olanzapine, a type of SGA known to cause non-classical obesity, was investigated through the expression levels of both genes and proteins of cannabinoid receptor 1 (CB1R) and melanocortin 3 receptor (MC3R), two proteins which had been implicated as important components in energy metabolisms (2,3). In this study, to further understand the underlying mechanism of olanzapine induced

weight gain, the drug was orally administrated to ten healthy Wistar-rats and then they were treated with metformin, which was known as anti-diabetic drug administered along with olanzapine, in various times. Next, the hypothalamic gene expressions´ and protein levels of those candidate genes were analyzed with RT-PCR and Western-blot analyses, respectively. While CB1R's gene expression was apparently not affected, MC3R's gene expressions were decreased in animals administered only with olanzapine, with a marked increase in animals administered with olanzapine coupled by metformin. The gene expression results of MC3R were complemented by the decreases detected in protein levels of MC3R from olanzapine-affected animals; along with marked recovery of protein expressions in animals administered by both olanzapine and metformin together. These results might serve as another clue in elucidating the exact mechanisms of SGAs on the development of metabolic disorders which would serve as another step in the developments of better antipsychotics in terms of both higher efficacies and lower side effects.

Keywords: obesity, antipsychotics, Cannabinoid Receptor 1, Melanocortin 3 receptor

ÖZ

SIÇANLARDA KANNABİNOİD VE MELANOKORTİN RESEPTÖRLERİNİN İFADE ÜZERİNE METFORMİN YÖNETİMİ İLE VEYA OLMAYAN OLANZAPİNİN ETKİLERİ

Jacob Alis, Aditya Kemal
Yüksek Lisans, Biyokimya, Biyokimya Bölümü
Tez danışmanı: Doç. Dr. Tülin Yanık

Ağustos 2017, 94 sayfa

İkincil nesil antipsikotiklerin (SGD) her iki etkinliklerinin açısından ilk nesil antipsikotiklerin (BKA) üzerinde bir gelişme olarak lauded, obezite ve diyabetik fenotipleri gibi metabolik yan etkiler azaltılmış (1). Bununla birlikte, İkinci kuşak yine BKA'lar kıyasla düşük şiddeti de olsa, yukarıda bahsedilen metabolik yan etkiler bir bolluk ile kalmışlardır. İKA'lar yan etkileri geniş bir farklı deneyler aracılığıyla araştırılmıştır birlikte, metabolik bozukluklar geliştirme İKA'ların mekanizması tam olarak tespit edilmemiştir. Deneyde olanzapinin etkiler, klasik olmayan obeziteye neden olduğu bilinen SGA bir tür, genler ve kannabinoid reseptörleri 1 (CB1R) ve melanokortin reseptörleri 3 (MC3R) proteinlerinin her ikisi de ekspresyon seviyeleri ile iki protein araştırılmıştır enerji metabolizması önemli bileşenler (2,3) olarak implike edilmiştir. Bu çalışmada,ayrıca, olanzapinin neden olduğu kilo alımı mekanizmasının anlaşılması, ilaç ağız yoluyla, on sağlıklı Wistar farelere uygulandı ve daha sonra,

çeşitli zamanlarda, olanzapin ile birlikte uygulanan anti-diyabetik ilaçlar olarak bilinen metformin, ile tedavi edildi. Daha sonra, bu aday genlerin hipotalamik gen expressions' ve protein düzeyleri RT-PCR ve Batı benek analizi ile analiz edilmiştir,sırasıyla. CB1R en gen ifadesi görünüşe etkilenmezken, MC3R en gen ifadeleri metformin ile birleştiğinde olanzapin verildiği hayvan belirgin bir artış ile sadece olanzapin ile uygulanan hayvanlarda düşmüştür. MC3R gen ekspresyon sonuçları olanzapinin-etkilenen hayvanların MC3R protein seviyeleri tespit azalmalarla tamamlanmaktadır; birlikte olanzapin ve metformin hem uygulanan hayvanlarda protein ifade belirgin iyileşme ile birlikte. Bu sonuçlar hem yüksek etkinliklerinin hüküm ve alt yan etkilere daha iyi antipsikotiklerin gelişmeler yeni bir adım olarak hizmet verecek metabolik bozuklukların gelişimine İKA'ların tam mekanizmaların tanıtılması başka ipucu olarak hizmet olabilir.

Anahtar kelimeler: obesite, antipsikotikler, Cannabinoid Receptor 1, Melanocortin 3 receptor

ACKNOWLEDGEMENTS

The author of this thesis would like to express his utmost gratitude to the following people. First of all, my gratitude for Assoc. Prof. Dr. Tülin Yanık as the supervisor of this project and the main source of guidance, inspirations, criticisms, insights, and supports throughout the research.

Next, I'd like to express my gratitude for Prof. Dr. Semra Kocabıyık, Prof. Dr. Fatih İzgü, Assoc. Prof. Çağdaş D. Son, and Asst. Prof. Dr. Süheyla Doğan Bulut who have graciously given their time as jury members from outside of campus during the thesis defense period.

Next, I'd like to give thanks for the members of Yanık laboratory, who have helped me during various stages of this experiment.

For my family, who keeps supporting my heart and mind through this experiment.

For my friends, who help me in everything, be it professional or personal matter.

TABLE OF CONTENTS

LIST OF TABLES

TABLES

LIST OF FIGURES

FIGURES

LIST OF ABBREVIATIONS

Δ^9-THC	Tetrahydrocannabinol
5-HT_2	Serotonin 2 receptor
2-AG	2-Arachydonoglycerol
AC	Adenylate cyclase
α-MSH	Alpha-melanocyte stimulating hormone
AMPK	Adenosine monophosphate kinase
BMI	Body mass index
Ca2+	Calcium ion
cAMP	Cyclic adenosine monophosphate
CB1R	Cannabinoid receptor type 1
cDNA	Complementary DNA
D2	Dopamine 2 receptor
ECS	Endocannabinoid system
FGA	First generation antipsychotics
γ-MSH	Gamma-melanocyte stimulating hormone
GPCR	G-protein coupled receptor

K+	Potassium ion
MC3R	Melanocortin 3 receptor
NPY	Neuropeptide Y
PAGE	Polyacrylamide gel electrophoresis
POMC	Proopiomelanocortin
PVDF	Polyvinylidene fluoride
SDS	Sodium dodecyl sulfate
SGA	Second generation antipsychotics

CHAPTER 1

INTRODUCTIONS

1.1. OBESITY

Obesity is a rising phenomenon in the modern era, especially in the developed countries and quite recently in developing countries (Kelly, et al., 2008). Obesity is characterized by the increase in body mass index (BMI), which leads to various disorders including but not limited to diabetes, cardiovascular diseases, cancer, and premature death (Haslam and James., 2005).

While the majority of obesity cases are caused by overconsumption, a significant proportion can be traced due to side effects of drugs such as antipsychotics, antidepressants, antianxiety, and antiepileptic (Breum and Fernstorm, 2001).Various antipsychotics are known to induce obesity among other metabolic disorders as side effects. Two generations of antipsychotics, namely the first and the second generations, are known to induce various metabolic disorders to their recipients. Among the disorders, significant weight gain through increased feeding rate and type-2 diabetes are among the most common (Rojo et al, 2015). Cardiovascular diseases are also another considerably important metabolic disorders caused by antipsychotics' administration (Bressington et al., 2016).

1.2. SECOND GENERATION ANTIPSYCHOTICS (SGAs)

SGAs are a category of drugs used in treating diverse mental complications such as schizophrenia and bipolar disorders. Developed as a replacement for first generation antipsychotics (FGAs), SGAs exercise their effects on various serotonin and dopamine receptors as antagonists. Several researches in meta-analysis have tried to point out the efficacy of SGAs compared to FGAs. One of the most recent researches utilized multi-analysis methods in meta-analysis experiment to compare the efficacies of SGAs compared to FGAs, and in many respects, SGAs outperformed both FGAs and placebo controls in terms of reduction of symptoms. However, this result was valid only for some SGAs, questioning the overall efficacy of the SGAs, although it was noticed that SGAs did have less adverse side effects compared to FGAs (Leucht et al, 2008).

1.2.1. Metabolic side effects of SGAs

Although they are designed to possess broader spectrum and less debilitating side effects than FGAs, SGAs are known to induce adverse side effects energy metabolism such as body weight and insulin sensitivity. The most prominent ones are weight gain and high feeding rate, which might lead to obesity, and type-II diabetes (Rojo et al, 2015). Potential side effect is type-2 diabetes mellitus, although the mechanisms are unknown at the moment. Other notable side effects include myocarditis, hyperlipidemia, and cataract (Ucok and Gaebel, 2008). A metabolomics analysis of serum metabolites in psychotic patients revealed an increase in lipid molecules associated with increased liver fat percentages (Suvitaival et al., 2016).

Clinically approved SGAs have been determined to cause variable changes in body weight. Among the most generally prescribed SGAs, olanzapine and clozapine were determined to be the ones causing the highest increase in body weight, even though they were also among the most efficacious SGAs currently prescribed (Figure 1). Risperidone, one of the SGAs with less severe weight gain, still caused significant BMI increase, along with decreasing leptin, NPY, and POMC's active form alpha-melanocyte stimulating hormone (α-MSH) expressions (Yanik et al, 2013).

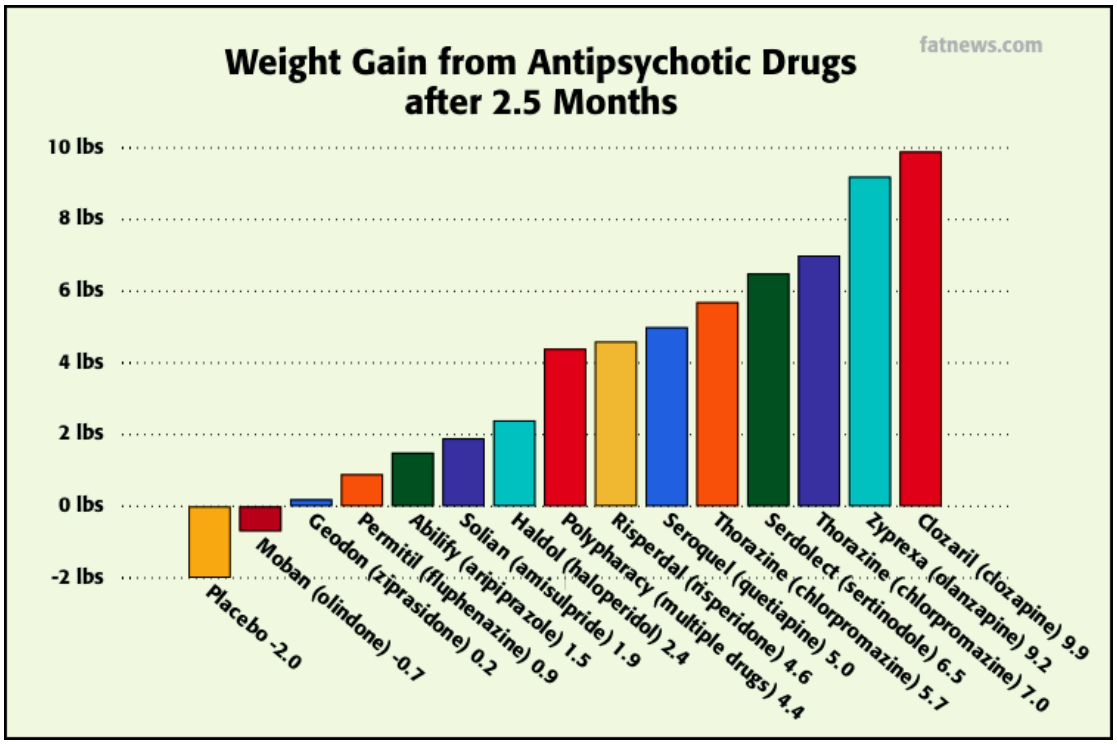

Figure 1. Weight gains recorded after anti-psychotics' administrations for 2.5 months in psychotic patients. Olanzapine and clozapine were among the most potent anti-psychotics; however caused most in weight again as averaged 4-5 kg after 2.5 months among patients (Newcomer, 2005).

1.2.2. Olanzapine and its efficacy

Olanzapine was developed as an atypical antipsychotic, a successor of FGAs intended to possess higher efficacy and less adverse side effects (Molecular structure

described in Figure 2). Olanzapine has affinity to many neuroreceptors such as 5-HT_{2A-C},3,6,7, dopaminergic D1–5, muscarinic M1–5, α1- adrenergic and histaminergic H-1 receptors (Bymaster et al 1997), however it exerts activity in blocking both dopamine D_2 and serotonin 5-HT_{2A} more prominently in mesolimbic pathway (Figure 3). For its body metabolism, it is handled primarily by cytochrome P450; with other mechanisms include CYP2D6 system, the flavin mono-oxygenase-3 system, and uridine 5′-diphosphate glucuronosyltransferases (UGTs) (de Leon et al 2005).

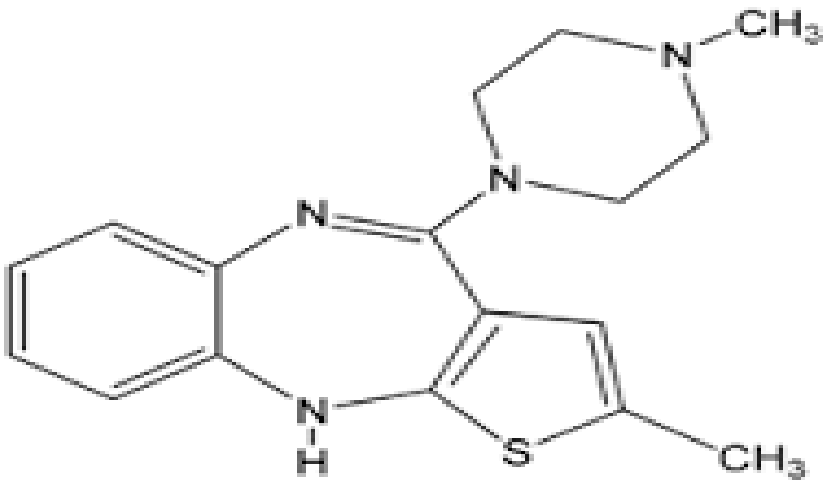

Figure 2. Olanzapine 2D structure (dailymed.nlm.nih.gov).

Many studies have documented the efficacy of olanzapine for treatment of different psychotic disorders. In 1999, one such study found that there was a significant improvement compared to placebo for treatment of patients with manic disorders (Tohen et al 1999). Other studies in 2002 placed olanzapine against divalproex in treating mania and olanzapine proved to be the more efficacious one (Baker et al, 2002; Zajecka et al, 2002). Another study tested the efficacy of olanzapine and olanzapine-fluoxetine Combination (OFC) against bipolar I depression and it showed that both performed significantly compared to placebo treatment (Vieta et al, 2003). It was also shown that the efficacy of OFC against lamotrigine, an approved medication

to treat bipolar disorder. The study revealed that OFC had both greater performance and less suicidal tendencies compared to lamotrigine (Brown et al, 2006).

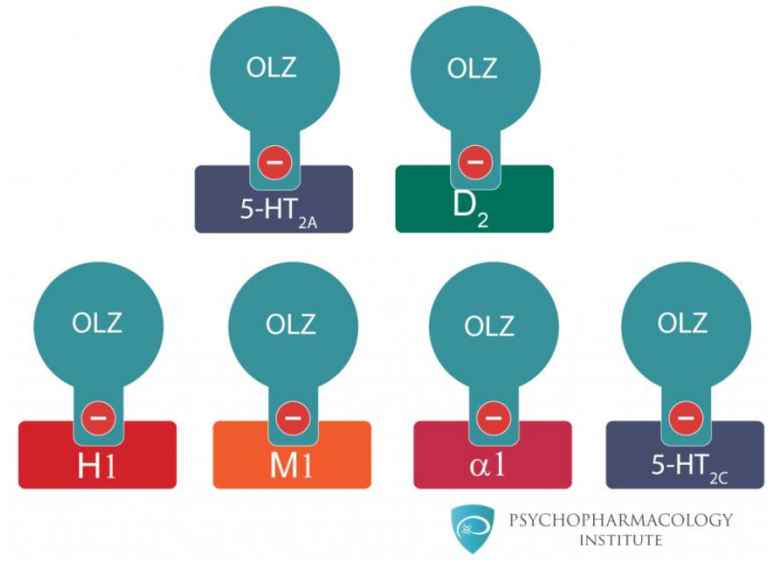

Figure 3. Olanzapine's inhibitions on different types of receptors. Dopamine-2 (D2) and serotonin-2A (5-HT2A) are the main targets, with secondary targets including histaminergic-1, muscarinic-1, adrenergic-1, and serotonin-2C receptors (Psychopharmacologyinstitute.com).

Figure 3. Olanzapine's inhibitions on different types of receptors. Dopamine-2 (D_2) and serotonin-2A ($5\text{-}HT_{2A}$) are the main targets, with secondary targets including histaminergic-1, muscarinic-1, adrenergic-1, and serotonin-2C receptors **(**Psychopharmacologyinstitute.com**).**

1.2.3. Side effects of olanzapine

Olanzapine has been documented to show many metabolic side effects, particularly weight gain. It is also one of the drugs that increase body weight the most among other antipsychotics tested (Bak, et al, 2014 and Haddad, 2005). Many researches have been initiated in order to unravel the mechanisms of this phenomenon. One study where male patients' body weight, BMI, NPY, and POMC were analyzed between pre-and post-treatment conditions was conducted in 2013. Post-treatment patient analysis revealed significantly heightened levels of body weight (amounting to 4.3 kg), BMI, NPY, and POMC's active form α-MSH after 20mg/day of olanzapine administration (AK et al, 2013). One of the most recent publications delved in the effect of ataxin-2 binding protein 1 (A2BP1)'s polymorphism on the antipsychotic-induced weight gain (AIWG). The experiment pointed that one of the single nucleotide polymorphisms (SNPs) of A2BP1 corresponded to AIWG caused by olanzapine (Dong et al, 2015). A newer research gave a new observation that olanzapine also caused a significant change in fatty acid compositions, namely the increase of saturated fatty acid proportions (Li et al, 2016).

1.3. METFORMIN AND ITS RELATIONSHIP WITH ANTIPSYCHOTICS.

Metformin (molecular structure in Figure 4) is a widely prescribed insulin sensitizer, which exerts its effects on energy metabolism through various actions; gluconeogenesis prevention by AMPK-dependent activation of key enzymes, whereas it also enhances glucose uptake and glycolysis using hexokinase and pyruvate kinase. Other locations where it might exercise its anti-metabolic dysfunction properties include muscle tissues where it activates AMPK actions and inhibits gluco- and lipotoxicity inflammation and adipose tissue through agonist-induced lipolysis inhibition and fatty acid oxidation stimulation (Diamanti-Kandarakis et al, 2010). A

study of the effects of metformin in treating Parkinson's disease revealed that metformin increased the expressions of brain region mitochondria-specific marker proteins and protected dopaminergic neurons and improved dopamine-sensitive motor performance (Kang et al, 2017).

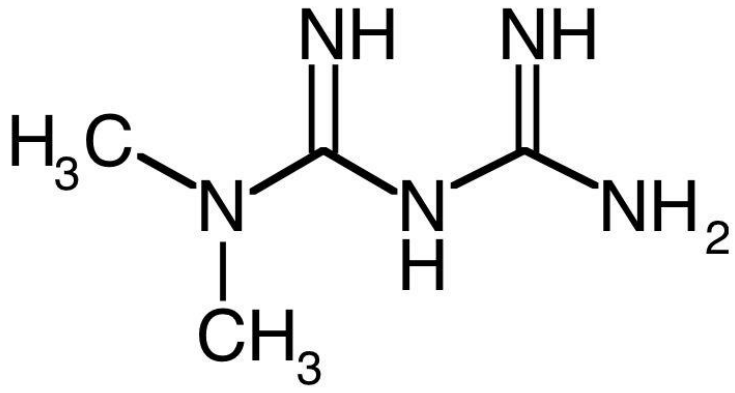

Figure 4. Chemical structure of metformin (Biohealthscience., 2013).

Metformin has been co-prescribed with various antipsychotic drugs in order to alleviate their metabolic side effects for weight gain and potential subsequent obesity. A case study involving feeding Sprague-Dawley rats with clozapine co-administered with metformin showed significant decrease in the insulin level compared to the clozapine and saline groups. And although the differences were not significant, there were slight differences of glucose transporter's (GLUT2) mRNA and protein expressions between the three groups (Gao et al., 2013). Another recent investigation involving utilizing hyperinsulinemic-euglycemic clamp (HIEC) to measure glucokinetics of olanzapine (3 mg/kg/day) pre-administered Sprague-Dawley rats after two sets of metformin dosage (150 mg/kg and 400 mg/kg of feed) were applied. Metformin managed to attenuate hepatic insulin resistance, but it failed to restore peripheral insulin sensitivity (Remington et al, 2015).

1.4. HYPOTHALAMIC METABOLISM CONTROL

Hypothalamus is involved in energy metabolism through its arcuate (ARC) nucleus control of feeding and energy usage. Four primary neuropeptides are divided into two groups in terms of their function upon feeding rate; agouti-related peptide (AgRP) and neuropeptide Y (NPY) increase feeding rate whereas proopiomelanocortin (POMC) products and cocaine-amphetamine related transcript (CART) reduces feeding rate (Figure 5). By controlling the feeding rate, these neuropeptides influence energy uptake of the body which leads to either increased or decreased body weight (Boswell and Dunn, 2017). These four peptides are directly controlled through the action of leptin, specifically inhibition of both AgRP and NPY's activities and promotion of both POMC and CART's activities (Panariello et al, 2012). Insulin also plays a huge role in regulation through its stimulatory effect on POMC and CART expressions and inhibitory effect on NPY and AgRP. By binding to its receptors located on POMC and CART-synthesizing neurons, insulin increases both POMC and CART synthesis. POMC and CART then binds to their receptors located on the NPY and AgRP-synthesizing neurons, causing inhibition on the synthesis of these products (Plum et al, 2017).

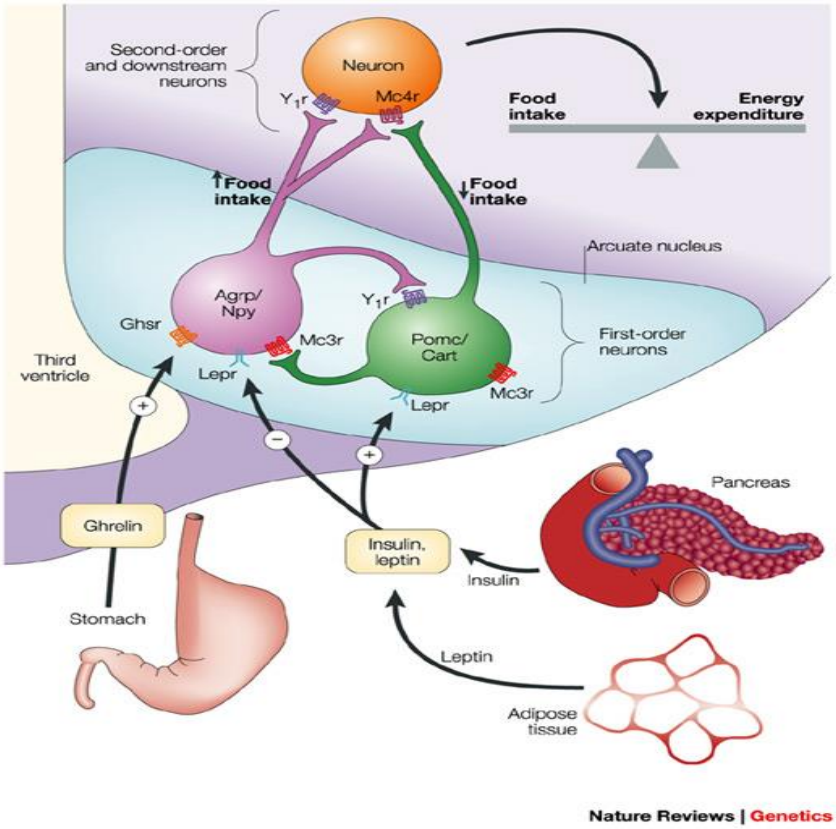

Figure 5. **The diagram showing the control mechanisms of ARC nucleus' neuropeptides on the energy metabolism and food intake.** POMC/CART and AgRP/NPY neurons reduce feeding rate and increase feeding rate, respectively. Their mechanisms are controlled through the actions of insulin/leptin and ghrelin (Barsh and Schwartz, 2002).

1.4.1. Antipsychotic's effect on arcuate nucleus' neuropeptides.

Researches regarding the effects of antipsychotic's administration on the expression level of these neuropeptides have been conducted extensively. Olanzapine administration was found to decrease POMC's mRNA and subsequently increase NPY's mRNA expressions. These changes were accompanied by the increases observed in body weight and adipose tissue amount (Lian et al, 2014). Other experiment about olanzapine administered in Wistar rats was seen to decrease mRNA expressions of various ARC neuropeptides, namely POMC, CART, and NPY, which accompanied increased body weight (Sezlev-Bilecen et al, 2016). Meanwhile,

risperidone which is another antipsychotic cause medium weight gain, also produced similar results in terms of body weights and POMC's mRNA expressions to those demonstrated by olanzapine-treated male Wistar rats (Kursungoz et al, 2015).

1.4.2. Other systems potentially related to the antipsychotics' side effects.

While some studies have been conducted to examine the effects of antipsychotics to the expressions of POMC, NPY, AgRP, and CART peptides which lead to increased body weight, other pathways have yet to be explored. This project would examine the effects of olanzapine on two other metabolic systems which were rarely explored. First one was endocannabinoid system (ECS), with cannabinoid receptor type 1 (CB1R) as the primary metabolic-related receptor. Second one was the melanocortin system which consists of receptors responsible in regulating feeding rate. Out of the receptors included in melanocortin receptor family, melanocortin receptor 3 (MC3R) would be the focus of the project.

1.5. ENDOCANNABINOID SYSTEM (ECS)

ECS is a collection of neurotransmitter lipids and their receptors. All endocannabinoids are eicosanoids; with a couple of examples include anandamide and 2-arachidonoyl glycerol. They are synthesized from cell membrane phospholipids and they are not stored in vesicles. Instead, they are rapidly degraded upon signaling cascade completion. Their receptors include CB1R and 2 (CB2R). Both receptors are G-protein coupled receptors; however the majority of receptor expressions' locations are quite different. CB1R is expressed mainly in neurons, particularly in central nervous system (CNS) region of forebrain, basal ganglia, cerebellum, hippocampus and cerebral cortex and also axons, neurons terminal, and astrocytes. CB2R is expressed in

immune cells, particularly in spleen, thymus, and circulating immune cells (Cota, 2007).

1.5.1. Function of ECS

ECS plays a large role in modulation of energy intake (Figure 6). Both endocannabinoid oral and injections have been shown to increase food consumption and preference to palatable food (Brown et al, 1977; Hao et al, 2000). Another experiment with CB1R $^{-/-}$ rats showed decreased food intake and leaner phenotype, along with reduced lipid and total body mass (Cota et al, 2003). It has also been shown that endocannabinoid system affects eating behavior through not only hypothalamus, but also through the circuitry of reward, which is a bundle of synaptically connected neurons from various brain areas (Gardner, 2005). Both endocannabinoid ligands anandamide and tetrahydrocannabinol (Δ^9-THC) have been shown to not only stimulate food intake but also increase the duration and bouts, suggesting behavioral modulation (Williams CM, Kirkham TC, 2002). Another aspect of ECS modulation is that it extends to peripheral metabolic organs and cannabinoid receptor 1 (CB1R) has been identified in many tissues related to metabolism, such as pancreas, gut, and liver (Cota, 2007). The evidence has been obtained using genetically modified obese rodent models where after administration of CB1 antagonists reduced food intake and weight loss, the latter seems to be permanent even after returning to normal feeding rate (Trillou et al, 2003).

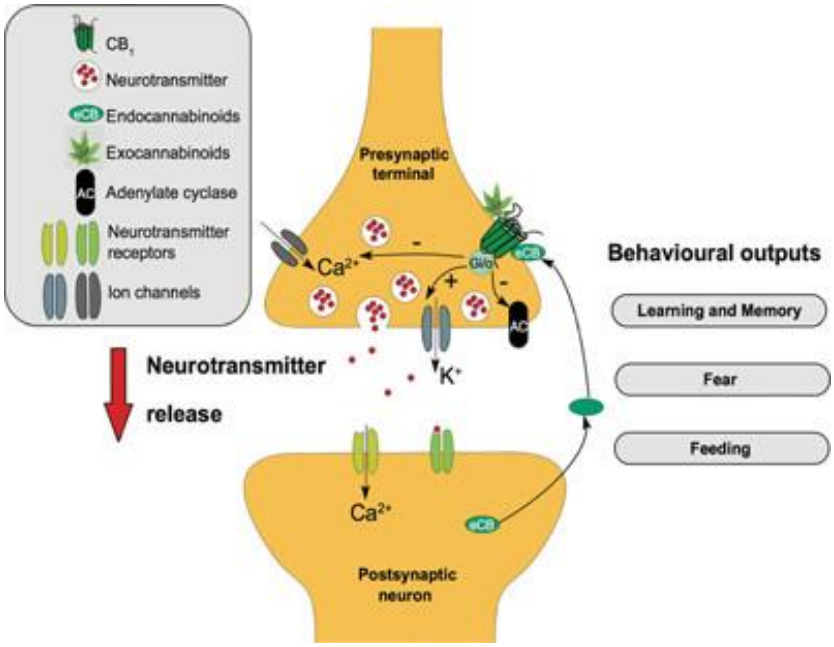

Figure 6. A diagram of endocannabinoid system (ECS). ECS affected various behavioral outputs, particularly feeding. Endocannabinoids and exocannabinoids synthesized by post-synaptic end of neurons stimulated Ca2+ intakes, neurotransmitter release, and inhibition of adenylate cyclase (AC) (Busquest-Garcia etal., 2015).

1.5.2. Endocannabinoid system and obesity

Endocannabinoid system has a significant role in modulating obesity phenotypes. Plasma levels of both endocannabinoid ligands anandamide and 2-Arachydonoylglycerol (2-AG) have been shown to be higher in obese women compared to lean women (Engeli et al, 2005). In fact, it seemed that both males and females diagnosed with abdominal obesity have higher concentration of 2-AG circulating (Bluher et al, 2006).

There are several hypotheses about the role of ECS dysfunction in obesity phenotype regulation. Stress might be one of the factors (Di et al, 2003), and diet consisting of long polyunsaturated fatty acids seems to increase the amount of endocannabinoids in the brain (Berger et al, 2001). Another factor worth considering is the polymorphism of several genes regulating ECS. One example is one polymorphism of a gene fatty acid amide hydrolase (FAAH), designated FAAH 385, which is an enzyme capable of inactivating most endocannabinoids. This particular polymorphism has been detected in higher frequency among individuals with higher than average body mass index (Sipe et al, 2005). One other research involving anorexia nervosa has been related to polymorphisms in Cannabinoid receptor 1 (CB1R) gene (Siegfried et al, 2004).

1.5.3. Cannabinoid receptor 1 (CB1R) as a part of ECS

CB1R is one of the two main cannabinoid receptors expressed in endocannabinoid system. It is a G-protein coupled receptor, and is highly expressed around the brain tissue in areas such as forebrain, basal ganglia, cerebellum, cerebral cortex, and hippocampus, along with fewer expressions, although highly efficient, in hypothalamus (Mailleux et al, 1992; Herkenham et al, 1991; Breivogel and Childers, 1998). It has been cloned from mice, rats, and humans and all of them exhibit 97 to 99 percent amino acid identity across species (Howlett et al, 2002). CB1R is also known to be expressed in symmetric, GABAergic synaptic boutons innervating NPY/AgRP neurons, and CB1R-containing neurons also project symmetric and asymmetric synapses to NPY/AgRP negative neurons (Morozov et al, 2017).

1.5.4. Mechanism of CB1R

When cannabinoid ligands bind to CB1R, it activates signaling cascade involving different enzymes and secondary messengers. Its activation separates Gi alpha subunits from beta/gamma subunits, and Gi alpha then proceeds to deactivate adenylyl cyclase. Inhibition of adenylyl cyclase in turn decreases cAMP concentration, which then inhibits protein kinase A. This inhibition then affects subsequent cellular processes (Howlett et al, 2002). Activation of CB1R also regulates different ion channels, such as activation of K+ channels (McAllister et al, 1999), inhibition of different types of voltage-gated Ca2+ channels (Gebremedhin et al, 1999; Pan et al, 1996; Mackie et al, 1995; Hampson et al, 1998), increases transient Ca2+ concentration (Sugiura et al, 1996), and regulation of focal adhesion point, MAP and PI3 kinases, and ceramide metabolism (Derkinderen et al, 1996; Wartmann et al, 1995; Gomez del Pulgar et al, 2000; Sanchez et al, 2001).

1.5.5. CB1R and obesity

Due to its effects in metabolism, CB1R has been a target for obesity treatment. Several CB1R antagonists have been developed in order to decrease body weight, reducing adipose tissue mass, and repairing glucose homeostasis. CB1R antagonists SR141716 and AM251 managed to decrease the weight of diet induced obesity (DIO) mice even after food intake level is returned to normal (Trillou et al, 2003; Hildebrant et al, 2003). In humans, the trial for CB1R antagonist Rimonabant managed to decrease the body weight up to 8.6 kg compared to 1.4-2.3 kg in placebo treatment over the course of 1 year (Van Gaal et al, 2005). Rimonabant was predicted to be acting on the metabolism of brown adipose tissue (BAT), Administrations of those antagonists also managed to decrease the adipose tissue mass in different body sites (Hildebrant et al, 2003), also indicated with reduction of waist circumference in these individuals

(Scheen et al, 2006). Another effect of this treatment is reduction of both total cholesterol and low density lipoprotein (LDL) levels of obese mice fed with high fat content diet (Poirier et al, 2005). Meanwhile, the level of high density lipoprotein (HDL) is increased following CB1R antagonist treatment (Despres et al, 2005) and this trend continues up to two years (Pi-Sunyer et al, 2006). Rimonabant, a well-known CB1R antagonist, is known to counteract the effects of obesity through increase of insulin sensitivity and the expressions of high voltage-activated calcium channels (HVACCs) and calcium channel v 1.1 (Cav1.1) (Chen and Hu., 2017). Figure 7 below showed proposed mechanism of how CB1R antagonist might lead to decrease in weight gain (Boon et al, 2014).

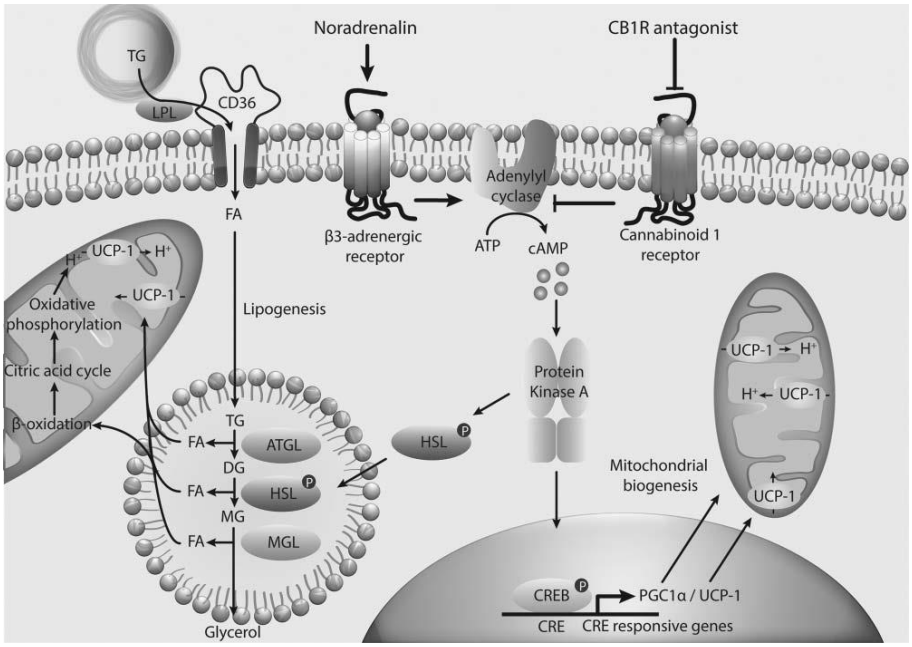

Figure 7. Proposed mechanism of how CB1R antagonists influence brown adipose tissue's activation. This leads to weight loss and decreased dyslipidemia, the two signs of obesity phenotype (Boon et al, 2014).

1.5.6. CB1R and its potential in antipsychotic research

Due to its effect in metabolism and that its antagonist produced commendable results in terms of treating obesity, cannabinoid receptor 1 seems to be a perfect candidate in research of the side effect caused by antipsychotics, such as olanzapine, which causes obesity phenotype to develop. One research discovered that olanzapine managed to in some way decreased the CB1R binding density in the DVC and ARC region of hypothalamus. It was outlined that other molecular signs of obesity, such as increased NPY mRNA concentrations, decreased POMC mRNA concentrations, and increased glutamic acid decarboxylase 65 (GAD65) mRNA concentrations. It was surmised that decrease in CB1R binding density results in less regulated cannabinoid-regulated GABA inhibition, resulting in increased of GABAergic response against POMC, lowering its concentration and encouraging weight gain **(**Weston Green et al, 2012**)**. It was claimed that CB1R gene polymorphisms are not involved in olanzapine-induced weight gain (Park et al, 2011).

1.6. MELANOCORTIN 3 RECEPTOR (MC3R)

MC3R is a part of melanocortin receptor family, a seven-subunit G-protein coupled receptor (GPCR) family which is a part of biological system responsible for energy metabolism of the body. Melanocortin family is comprised of five receptor types, ranging from melanocortin one (MC1R) to five (MC5R).

Out of the five, MC3R and MC4R are the two receptors related in the appetite regulation, satiety, and food preference. MC3R is expressed primarily in POMC neurons, just like the MC4Rs. MC3R is also activated by POMC's active forms, α-, β-, and *γ*-melanocyte stimulating hormone (MSH). MC3R has particular affinity to *γ*-MSH compared to MC4R and MC5R (Grieco et al, 2000). This particular affinity is evidently managed by the C-terminal residue of *γ*-MSH, which a particular isoform *γ2*-MSH, the

one with the highest affinity with the receptor (Joseph et al, 2010). In terms of function, MC3R is known to be responsible in management of feeding behavior in terms of anticipatory patterns of activity and wakefulness during limited nutrient availability (Sutton et al., 2008).

MC3R works through coupling with different intracellular subunits to execute different functions. First, Gαβγ signaling after MC3R ligand binding leads to PKC and IP_3 activations. Meanwhile, Gαs subunit activates cAMP/PKA pathway, to activate protein kinase A (PKA) to inhibit calcium ion signaling. Lastly, Gαi activates PI3K to induce cell proliferation (Figure 8).

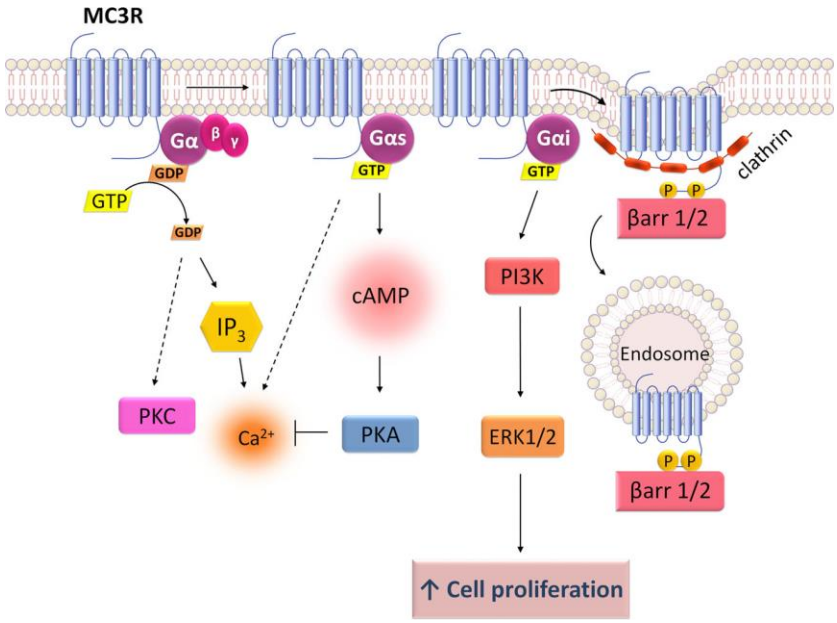

Figure 8. Mechanism of MC3R related to both calcium signaling and the cell proliferation. MC3R works with G subunits to exert the effects of ligands, from Calcium signaling to cell proliferation. As of now, the complete relationship between MC3R and weight gain have yet to be discovered (Rodrigues et al, 2014).

1.6.1. MC3R deficiency on energy metabolism

MC3R deficiency has a particular effect on the metabolism of the body. Like MC4R-deficient mice, there are signs of obesity; albeit with a different phenotypic observation. An older observation of MC3R -/- mice over the course of 4-6 months revealed increased fat mass, reduced lean mass and higher feeding efficiency, accompanied by higher leptin concentration and normal metabolic rates (Chen et al, 2000). MC3R knockout also caused the paradoxical weight gain with reduced feeding rate, which might be attributed to defective fasting-induced white adipose tissue lipolysis, fasting-induced liver triglyceride accumulation, fasting-induced refeeding, and fasting-induced regulation of the adipostatic and hypothalamic-adrenal-pituitary axes (Renquist et al, 2012).

Contrary to the MC4R which has been extensively studied and characterized, there have been only a few investigations to the effects of MC3R's alterations on the body weight and metabolism. Attempts on rescuing MC3R phenotype through DAT-MC3R, a type of Cre-recombinase system which is controlled by endogenous dopamine transporter promoter (Horizon Labs, 2017) did not re-establish food self-administration and nutrient partitioning phenotype (Mavrikaki et al, 2016).

1.7. HYPOTHESIS AND AIM

1.7.1. Hypothesis

Based on the aforementioned information in the introduction, the hypothesis was formulated. Our hypothesis could be separated to two points:

- Given the effect of CB1R's dysfunction on weight gain, it was hypothesized that CB1R's expression would increase through olanzapine administration.

- As for MC3R's expression, it was thought that the decrease on olanzapine-administered groups would be detected.

1.7.2. Aim

After the hypothesis was determined, project's aim was set along these lines:

- First objective would be the determination of genes' expressions through the means of real time polymerase chain reaction (RT-PCR) as a relative quantification measurement method of the expressions.
- Second objective would be the determination of receptors' expressions by the means of western blotting, followed by proteins' relative quantification measurements.

CHAPTER 2

MATERIALS AND METHODS

2.1. Animal Materials

Total RNA amples were obtained from a group of male Wistar rats from the previous experiment (Kurt, 2014) in our lab. All RNA samples were already subjected to DNAse treatment and cleaning procedure. Before PCR and RT-PCR treatment, each sample was tested with agarose gel electrophoresis in order to determine their health (Figure 1). The 28S, 18S, and 5S bands were used as the indicators of theRNA conditions. The RNA samples were separated according to the treatment of rats applied as follows:

- Control group1 (CTRL1): This control group was not treated by any drug for 14 weeks
- Control group (CTRL2): This control group was treated by anti-diabetic drug metformin (Dosage: 250mg/kg/day) in drinking water for the last seven weeks.
- The first olanzapine group (OLA1): The rats were administered olanzapine (Dosage: 4mg/kg/day) in 10 percent sucrose solution for 14 weeks.
- The second olanzapine group (OLA2): The rats were first administrated olanzapine for 7 weeks. After 7 weeks, olanzapine coupled with metformin was administered.

- The third olanzapine group (OLA3):The rats were administered olanzapine coupled with metformin from the start for 14 weeks

For the protein samples, total hypothalamic protein was isolated after surgery from the Wistar rats. Extraction protocol was derived from TRIZOL protocol originally used to extract RNA (BMC Genomics, 2013).

2.2. Total RNA concentration determination with NanoDrop.

NanoDrop (Cambridge, UK) was utilized for determination of RNA concentration. Also, for intact RNA 260/280 nm wavelength ratio would be expected to be 2,0 while 260/230 nm wavelength ratio would be expected to be around 1,8 – 2,2 (Thermo Scientific, 2009).

2.3. Complementary DNA (cDNA) synthesis materials and methods

Kits were purchased from various suppliers. The RevertAid First Strand cDNA Synthesis Kit, Thermo Scientific (Waltham, MA, USA) (catalog #K1622) was utilized for cDNA synthesis. With the exception of 10X dNTP mix, all the materials required were included in the kit module (10X dNTP mix was purchased separately from the same supplier). For the tools, 0,2 - 10 µL and 2 – 200 µL tips with appropriate Thermo Scientific pipettes were utilized, as well as BIO-RAD T100 Thermal Cycler (Singapore City, Singapore) as the incubator. Table 14 in appendix listed reagents required with their concentrations.

cDNA synthesis procedure was divided into two phases. In the first phase, mRNA strands and random hexamer primers were added to 0,2 µL PCR tubes and heated up to 65^{o}C in order for the strands and primers to anneal with each other. To keep the cDNA

total concentration in the range of 500 nM/µL, the mRNA's final concentration was to be adjusted, along with the final concentration of nuclease free water (NFW).

The second phase reagents were included after the short incubation. 4 µL of Thermo Scientific's 5X Reaction Buffer was added as the buffer required for the enzyme to function. Then 2 µL of 10 mM dNTP was added as the building blocks for the synthesis procedure. To prevent mRNA degradation by RNAse, RiboLock RNAse inhibitor was then added to the tubes. Finally, RevertAid Reverse Transcriptase, the main enzyme which converts RNA to complementary DNA strands, was added last (Table 1).

cDNA synthesis protocol was conducted in BioRad T1000 thermal cycler, using its incubation function. Initiation phase is conducted at 65^{o}C for 5 minutes to let both mRNA strands and primers anneal with each other. After adding the reagents from the second phase, the tubes were incubated at 25^{o}C for 5 minutes to activate the reverse transcriptase enzyme. Synthesis step was next to be initialized, where the mixture was incubated at 42^{o}C for 1 hour to let the enzyme synthesizes cDNA strands out of mRNA fragments. Finally, termination step was conducted at 70^{o}C to prevent excessive cDNA synthesis. Table 1 described the overall protocol.

Table 1. cDNA heating and duration protocol.

Procedure	Temperature	Duration
Initiation	65^{o}C	5 min
Incubation (after adding reagents from 2nd phase)	25^{o}C	5 min
Synthesis	42^{o}C	60 min
Termination	70^{o}C	5 min

2.4. Thermal gradient PCR materials and methods.

For PCR synthesis, kits from Thermo Scientific and Sigma-Aldrich (city, country) were utilized. PCR protocols were adapted from the manual guide of the kits, with slight alteration in initial denaturation and final extension, for both their temperatures and durations using Bio-Rad thermal cycler (Singapore City, Singapore)..

Reagents of PCR were added to 0,2 mL PCR tubes. First, 10X PCR buffer of 5 µL were added. Next, 10 mM dNTP mix of 1 µL was added. Next, both forward and reverse primers were added in order to provide the polymerase a definite starting point for cDNA fragment amplifications. 2,4 µL of 25 mM $MgCl_2$ was added as the catalyst of the Taq polymerase. Next, NFW was added, followed by the cDNA strands. Finally, the enzyme Taq polymerase was added as the last component of PCR procedure. Reagents and their appropriate concentrations were listed in Table 17 in appendix

Both forward and reverse primers of CB1R and MC3R were used as a way to specify intended fragment's amplification lengths. Forward primer sequence was 20 base pair in length, which was equal to reverse primer's length. The resulting fragment after amplification of CB1R would be measured to 94 base pairs (Figure 10). Similarly, MC3R primer set was also utilized in order to specify the fragment of the intended gene's length. The MC3R fragment's size is at 123 base pairs (Figure 18).

Initial denaturation was performed at 95 ^{o}C for 10 minutes in order to both activate Taq polymerase and denature DNA fragments from double stranded to single stranded form so primers could bind to the specific point of the gene. Another round of denaturation at 95 ^{o}C is performed for 30 seconds. For gradient PCR's annealing temperatures, two sets of temperature range between 65^{o}C - 55^{o}C (CB1R) and 57^{o}C - 47^{o}C (MC3R) were prepared for 8 tubes each; with every tube having its own. This was done to select the best annealing temperature for the CB1R and MC3R genes for the Real time polymerase chain reaction (RT-PCR) procedure. Extension procedure which allows Taq polymerase to amplify the selected genes of interest was then conducted at 72^{o}C for 30 seconds, which was an appropriate duration for our fragment length of 94

base pairs. Denaturation, annealing, and extension procedures were then repeated for 40 times, which was ended with final extension at 72^{o}C for 5 minutes and incubation at 4^{o}C indefinitely. Table 2 below listed the specific protocol for the thermal cycler.

Table 2. CBIR and MC3R gradient PCR protocol

Protocol Steps	Temperature	Duration
Initial Denaturation	95^{o}C	10 min
Denaturation	95^{o}C	30 sec
Annealing (CB1R)	65^{o}C - 55^{o}C	30 sec
Annealing (MC3R)	57^{o}C - 47^{o}C	30 sec
Extension	72^{o}C	30 sec
Final Extension	72^{o}C	5 min
Incubation	4^{o}C	Indefinitely
Cycles		40 times

2.5. CB1R and MC3R expression PCR.

After annealing temperatures for both CB1R and MC3R mRNAs were determined, expression PCR was conducted in order to determine that each samples contained both mRNA fragments. While the materials and the amounts were similar to those used for gradient PCR, however the annealing temperature and denaturation duration were slightly altered.

Initial denaturation was performed at 95 ^{o}C for 10 minutes in order to both activate Taq polymerase and denature DNA fragments from double stranded to single stranded form so primers could bind to the specific point of the gene. Another round of denaturation at 95 ^{o}C was performed for 30 seconds. Annealing temperatures for CB1R (59,7^{o}C) and MC3R (54^{o}C) were determined. Extension procedure which allowed Taq

polymerase to amplify the selected gene of interest was then conducted at 72^{o}C for 30 seconds, which was an appropriate duration for our fragment length of 94 base pairs. Denaturation, annealing, and extension procedures were then repeated for 40 cycles, which was ended with final extension at 72^{o}C for 5 minutes and incubation at 4^{o}C indefinitely. Protocols were listed in Table 3 below.

Table 3. CBIR and MC3R expression PCR protocols

Protocol Steps	Temperature	Duration
Initial Denaturation	95^{o}C	10 min
Denaturation	95^{o}C	30 sec
Annealing (CB1R)	59,7^{o}C	30 sec
Annealing (MC3R)	54,1^{o}C	30 sec
Extension	72^{o}C	30 sec
Final Extension	72^{o}C	5 min
Incubation	4^{o}C	Indefinitely

2.6. Real time Polymerase Chain Reaction (RT-PCR) materials and procedure.

For RT-PCR procedure, it would be divided to two steps. First, standard curves for each gene were generated. Second, the RT-PCR of those genes were conducted. For both standard curve procedure and gene of interest's RT-PCR synthesis, Sigma-Aldrich kits were utilized. Instead of 50 µL reaction, it was decided that 20 µL would be sufficient for the reaction. Optimization for each primers was performed using gradient PCR using PCR kits of previous experiments. For RT-PCR procedure, the main solution was Sigma-Aldrich's 10x SYBR GREEN Mix (Sigma-Aldrich, St. Louis, USA), which contains both Taq polymerase and SYBR GREEN dye, which would intercalate with double-stranded DNA fragments. After binding, the DNA fragments would be read with a quantitative cycler with photo sensors capable of reading the wavelength emitted by SYBR GREEN-DNA combination. This information would

then be converted to numerical data with specific software corresponding to the type of thermal cycler used. All the procedure steps were done in ice.

Firstly, NFW was added as the solvent for all the components. Next, primers were once again added in order for the enzyme to amplify only the specific fragment that we required. As the catalyst for Taq enzyme, 25 mM $MgCl_2$ was once again added. Complementary DNA (cDNA) fragments were added last. Below, Table 4 containing the materials with the appropriate concentrations was described.

Table 4. CB1R and MC3R RT-PCR reagents.

Materials	Volume per PCR tubes
10x SYBR GREEN Mix	10 µL
Forward primers (4 µM concentration)	1 µL
Reverse primers (4 µM concentration)	1 µL
25 mM $MgCl_2$	2,4 µL
CDNA (0,5 µM)	2 µL
NFW	3,6 µL
Total	20 µL

2.6.1. CB1R and MC3R RT-PCR standard curve procedure

Before the RT-PCR analysis, it was imperative that a standard curve for both genes was created in order to determine the quantification values. To do this, the samples were diluted up to 5 orders of magnitude, then ran the RT-PCR in duplicates for 40 cycles. The results were then analyzed using Corbett's ROTOR-GENE Q6000 software.

Serial dilution was required to create an appropriate standard curve for both CB1R and MC3R's RT-PCR procedures. This standard curve would be used to determine the relative quantification of the gene in RT-PCR determination. The dilution was set that

the succeeding tube will contain a tenth of the preceding cDNA concentrations. The dilution was repeated 4 times, resulting in the last tube containing a ten thousandth of the first tube's cDNA concentration. Serial dilution arrangement was listed in Table 5.

Table 5. Serial dilution arrangement.

Tube arrangements (x2)	Reaction volume (µL)
1x dilution	20
10x dilution	20
100x dilution	20
1000x dilution	20
10000x dilution	20

2.6.2. Gene of interest's RT-PCR materials and procedure

After the expressions of both CB1R and MC3R had been determined in all samples, RT-PCR in order to determine the exact numerical value of the expressions of both genes between control and olanzapine/olanzapine-metformin treated groups was performed. For this part of the experiment, once again the total reaction was 20 µL per PCR tubes, and this time the reaction was performed using Corbett's thermal cycler (Corbett, UK) quantitative thermal cycler. Reactions were then run in duplicates for both control (CTRL1, 2) and olanzapine-treated (OLA1, 2, 3) groups.

For RT-PCR procedure, Corbett thermal cycler machine was utilized. As with both gradient and expression PCR, the RT-PCR procedure also consisted of initial denaturation, denaturation, annealing, and extension. The difference was that melting temperature curve is added between 50^{o}C-99^{o}C. Melting temperature corresponded to the point where non-denatured and denatured DNA fragments are at 50/50 ratio. This was a useful feature to determine the purity of the samples. The procedure for

denaturation, annealing, and extension is again repeated for 40 cycles. The list of steps was presented below in Table 6.

Table 6. CB1R and MC3R RT-PCR protocol.

Protocol Steps	Temperature	Duration
Initial Denaturation	95^{o}C	10 min
Denaturation	95^{o}C	30 sec
Annealing (CB1R)	59,7^{o}C	30 sec
Annealing (MC3R)	54,1^{o}C	30 sec
Extension	72^{o}C	30 sec
Melting Temperature	50^{o}C-99^{o}C	13 min
Cycles		40 times

2.7. RT-PCR quantification analysis

For the analysis, Ct values for CB1R and MC3R of both control and treated groups were analyzed with the Qiagen ROTOR-GENE Q6000 software. For the equation, Liwak et al (2001)'s equation was utilized.

$$\Delta Ct = Ct\ (target\ gene) - Ct\ (reference\ gene)$$

$$\Delta\Delta Ct = \Delta Ct\ (treatment) - \Delta Ct\ (control)$$

$$Ratio\ (fold\ change) = 2^{-\Delta\Delta Ct}$$

2.8. Statistical analysis

For statistical analysis of the results, GraphPad Prism 5.0 software was utilized. Analysis of the results was performed using one-way ANOVA, accompanied with Tukey's test for correlation between groups, with parameter including P value <0,05.

2.9. Protein samples and Bradford assay material for the determination of total protein concentrations.

Protein samples were obtained from the same groups of both control and treated rats, separated to similar groups (Table 13 in Appendix). Total protein concentrations were determined by Bradford assay, which kit was supplied by Thermo-Scientific (Rockford, USA). Microplates were used to hold both Bradford reagent and protein samples. Spectrophotometer was supplied by Thermo-Scientific (Vaatan, Finland).

2.10. Western blot assay materials for the total hypothalamic protein samples.

Both separating and stacking gels were self-manufactured from various components available in the laboratory, which the compositions were listed in the Table 17. For antibodies, both primary and secondary antibodies were obtained from different companies, with MC3R primary antibody bought from Santa Cruz (Dallas, Texas, USA), while secondary antibody was bought also from Santa Cruz, (Dallas, Texas, USA). All the buffers were also self-manufactured from the available components, and they were listed in the Table 18 (Appendix). All necessary materials and procedure were adapted from the article detailing the western blotting procedure from 2012 (Mahmood and Yang, 2012).

Protein analysis was performed using western blotting procedures which are divided into two stages: running the protein samples mixed with 4x protein loading dye with 3:1 sample:dye ratio in SDS-PAGE gel electrophoresis and transferring the run samples from the gel to a polyvinylidene fluoride (PVDF) membrane which will be incubated with both primary and secondary antibodies. The thorough procedure was listed in Appendix B section.

CHAPTER 3

RESULTS

2.11. RNA quality determination.

The indicator for RNA quality control was the strong presence of the bands at 28S, 18S, and 5S positions. The gel picture of total RNA conditions from CTRL1, CTRL2, OLA1, OLA2, and OLA3 was shown in Figure 9. The RNA condition of those three samples was compared using 2X RNA ladder on the left. The RNA conditions, therefore, could be determined as quite healthy, given the bands' strength in all three size indicators seen below on the picture.

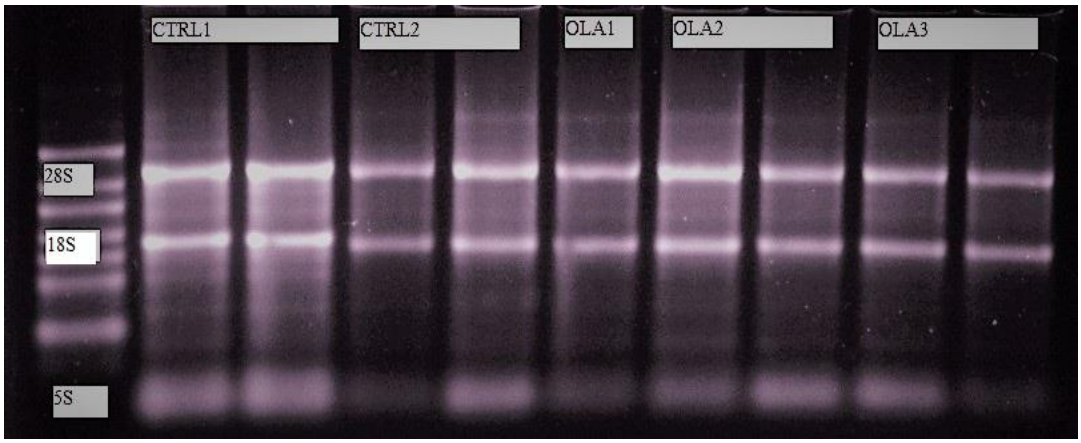

Figure 9. RNA sample quality control. The groups CTRL1, CTRL2, OLA1, OLA2, and OLA3 were used as the representatives of CTRL and OLA groups. The three brightest bands for each column represent 28S, 18S, and 5S RNA.

2.12. CB1R gradient PCR analysis.

To determine the appropriate CB1R annealing temperature, gradient PCR was performed. The sample used was the control group C1R2 for gradient PCR procedure. The result was analyzed through agarose gel electrophoresis. The gel picture showed that temperatures 59.7 and 57.8 ^{o}C was the best temperature for the primers to attach themselves to the gene of interest for amplification purposes. This observation was strengthened by the lack of non-specific amplification shown by the lack of bands in other places than the intended fragment size (Figure 10).

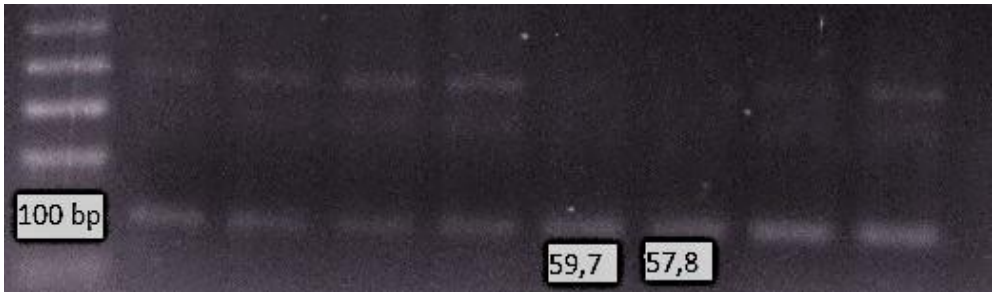

Figure 10. CB1R gradient PCR analyses. The left side represented DNA ladder, and the 100 bp label indicated the specific position closest to our intended cDNA fragment size, which is 94 bp. The columns represented the amplifications on different annealing temperatures, with the labelled temperatures (59,7 and 57,8 ^{o}C) giving the most specific amplifications.

Figure 10. CB1R gradient PCR analyses. The left side represented DNA ladder, and the 100 bp label indicated the specific position closest to our intended cDNA fragment size, which is 94 bp. The columns represented the amplifications on different annealing temperatures, with the labelled temperatures (59,7 and 57,8 ^{o}C) giving the most specific amplifications.

2.13. CB1R expression PCR.

After the melting temperature has been established, expression PCR was performed to compare both CTRL and OLA groups. Agarose gel electrophoresis was performed for visual confirmation. As the representatives of control groups, CTRL2 (no drug exposure) was chosen, while for the treated groups, OLA2 (olanzapine for the first 8 weeks, olanzapine coupled with metformin for the remaining 6 weeks) group was picked (Table 1). The leftmost part of the gel is reserved for DNA ladder of low base pair size, ranging from 25 – 1000 base pairs.

Figure 11 showed the comparisons of CB1R expressions between CTRL2 and OLA2 groups. The bands were aligned in the 100 bp level, which corresponded to the 94 bp fragment size of CB1R amplification from the selected primer (Table 4). Based on the figure, the specificity of the primers was shown by the observation that the bands forming on the same level, both in CTRL2 and OLA2.

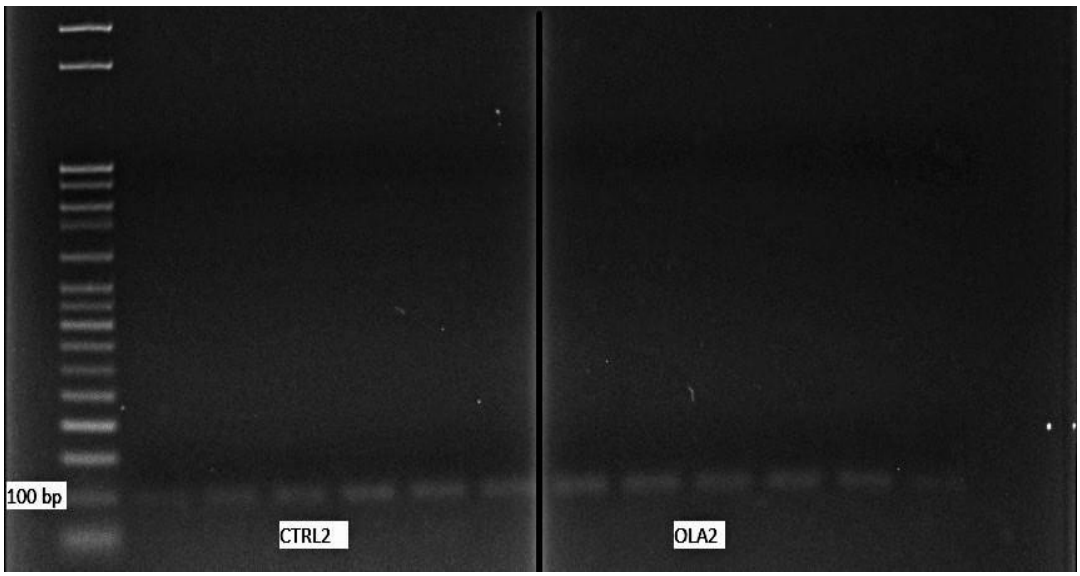

Figure 11. CTRL2 vs OLA2 CB1R mRNA expressions comparisons. The CTRL2 contained 6 groups, as did OLA2. The left part represented the ladder. The specific amplification indicated that all groups only amplified CB1R fragment at 94 bp size.

2.14. CB1R standard curve.

Before initiating RT-PCR, standard curve was created for fluorescence quantification. Standard curve is necessary in order to determine the relative quantification of olanzapine-treated groups when compared to the control groups. For the standard curve, control sample C4R1 of CTRL2 group was utilized as cDNA sample for RT-PCR standard reaction. In thermal cycler, the standard configuration was selected, which then measured relative quantification based on dilution level of the sample.

Figure 12 described the standard curve of CB1R quantification. For this curve, C4R1 sample was put through a series of increased dilution until the final sample's concentration was 1:10000 of the original concentration. The diluted samples were then run in thermal cycler on duplicates. After the run was over, we looked at the efficiency value to determine whether the curve is valid for use. The determination of the validity for the standard curve is based on the curve's efficiency. Standard curve's efficiency was determined to be 1,09. This value was located between 0,90 and 1,10, the acceptable range for RT-PCR standard curve.

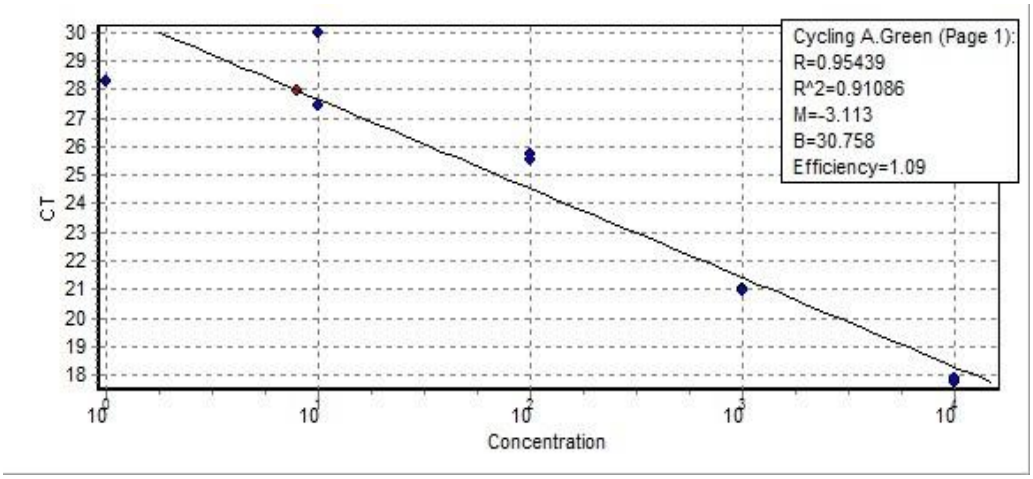

Figure 12. CB1R RT-PCR standard curve. The amplification efficiency was recorded at 1,09, which is between the acceptable range between 0,90 to 1,09 in terms of efficiency. The samples were run in duplicates, with dilutions 1/1, 1/10, 1/100, 1/1000, and 1/10000 with one copy of NTC.

2.15. CB1R RT-PCR analysis.

After standard curve was created, RT-PCR analysis on all samples from both control and treated groups was performed. Analysis of RT-PCR involves counting the Ct values of the samples and the melting curve of the reaction. Ct value was the intersection between an amplification curve and the threshold line, which could also be interpreted as the minimum number of cycles required to surpass the threshold level (background fluorescence) of the target gene. A smaller Ct value was inferred to correspond to the larger amplification concentrations. On the other hand, melting curve is a point where the ratio between bound and unbound primer to the target DNA fragment is 50:50. The curve is used to determine the purity of the sample and reagents used in the RT-PCR. And peak numbers determine the specificity of the primers used in the reaction. A single peak for all samples is the indicator that the primer binds only to our intended DNA fragment.

Figure 13 listed the melting curve of the CB1R RT-PCR from CTRL1 group as the representative for the control groups. The samples were run in duplicates, similar to RT-PCR gradient experiment. The total number of samples run was 20 duplicates, given that there were 10 samples in CTRL1 group. Along with the duplicates, one no-template control (NTC) was also run as the negative control of the experiment. As seen on the curve below, there was only one sharp peak which was formed by the samples, indicating that the primers bind only to the CB1R gene fragment.

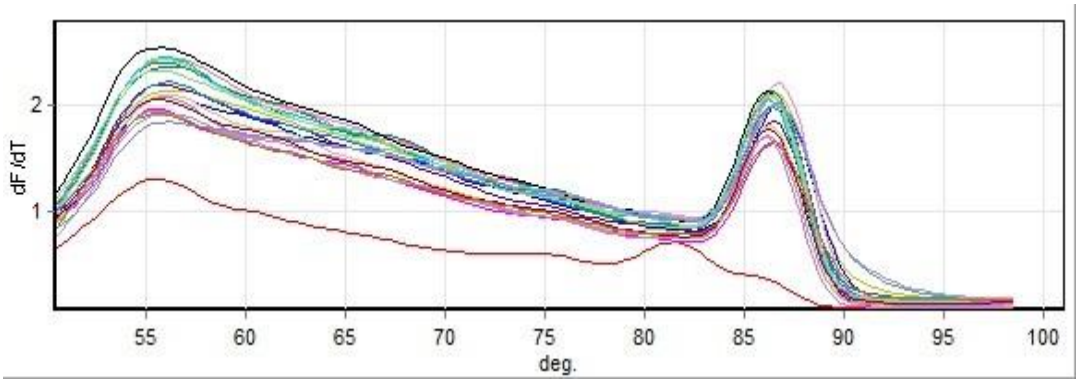

Figure 13. CB1R RT-PCR melting curve of CTRL1 group. Melting curve is established as way to determine the fidelity of RT-PCR. Convergence of peaks at the single point indicated that the primers were specific to the fragment.

Meanwhile, the melting curve of the CB1R RT-PCR from OLA2 group as the representative for the treated groups was shown in Figure 14 below. Similarly, the samples were run in duplicates, for the total of 20 duplicates of 10 samples. Along with the duplicates, one no-template control (NTC) was also run as the negative control of the experiment. The experiment also yielded one peak for all the duplicates, which again indicated the specificity of the primers for CB1R gene used.

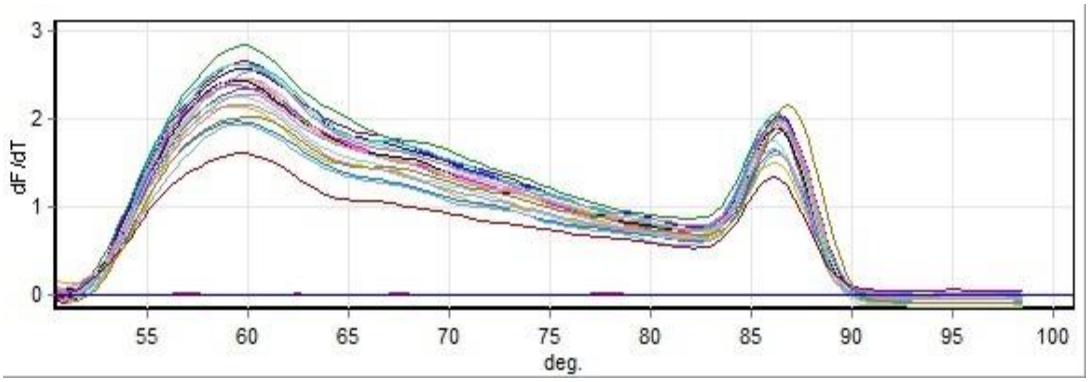

Figure 14. CB1R RT-PCR melting curve of OLA2 group. Melting curve is established as way to determine the fidelity of RT-PCR. Convergence of peaks at the single point indicated that the primers were specific to the fragment.

Table 8 below described the relative fold Ct values of each group when compared to one of the control groups. The relative fold Ct values will be the value used to determine the relative gene expression of control and treated groups. The values were derived from the average of the groups, which were then calculated using the equation derived from Liwak, 2001:

$$\Delta Ct = Ct\ (target\ gene) - Ct\ (reference\ gene)$$

$$\Delta\Delta Ct = \Delta Ct\ (treatment) - \Delta Ct\ (control)$$

$$Ratio\ (fold\ change) = 2^{-\Delta\Delta Ct}$$

The maximum value for the control is one, and from there the values for other groups will be determined. The values of each group depending on the control used were listed on table 7.

Table 7. Relative fold Ct values with comparison to different controls.

	CTRL1	CTRL2	OLA1	OLA2	OLA3
Fold Ct values (CTRL1)	1	0,2	0,16	0,26	0,31
	CTRL1	CTRL2	OLA1	OLA2	OLA3
Fold Ct values (CTRL2)		1	0,65	1,08	1,29
	CTRL1	CTRL2	OLA1	OLA2	OLA3
Fold Ct values (OLA1)			1	1,63	1,96

2.16. Fold ratio graphs for comparison.

After the relative Ct values of each group were determined, the values were listed in graphs below. Each graph had a different control used as the standard for relative Ct value comparisons. Therefore, the groups' values would change depending on the

control used. Figures 15, 16, and 17 listed the relative Ct values comparison compared to standards CTRL1, CTRL2, and OLA1 groups, respectively.

Figure 15 described the relative fold Ct values of each group when compared to CTRL1 as the standard. CTRL1's fold Ct values, the standard for this graph, was at 1, CTRL2's at 0,2, OLA1's (olanzapine-only) at 0,16, OLA2's (olanzapine-only for the first eight weeks, then metformin was applied together with olanzapine for the remaining six weeks) was at 0,26, OLA3's (olanzapine and metformin co-applied) at 0,31. The graph shows that CTRL1's value was the highest, and that the OLA1 group, the one where olanzapine was administrated solely, had the lowest value.

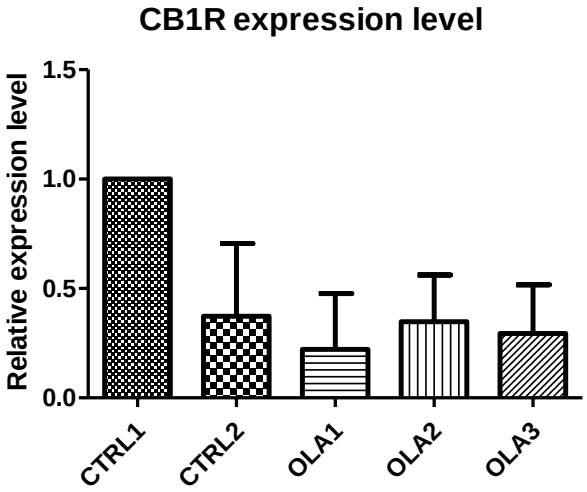

Figure 15. Fold Ct values of each groups according to CTRL1´s expression. As denoted by legend from left to right; CTRL1, CTRL2, OLA1, OLA2, and OLA3. –axis denoted relative expression levels of other groups in comparison to CTRL1.

Figure 16 showed the data where the CTRL2's value was used as the standard for measuring relative quantification of the groups. CTRL2's fold Ct values, the standard for this graph, was at 1, with OLA1's at 0,65, OLA2's at 1,08, and OLA3's at 1,29. In this figure, this time OLA3 had the highest relative value, whereas OLA1's value was once again the lowest.

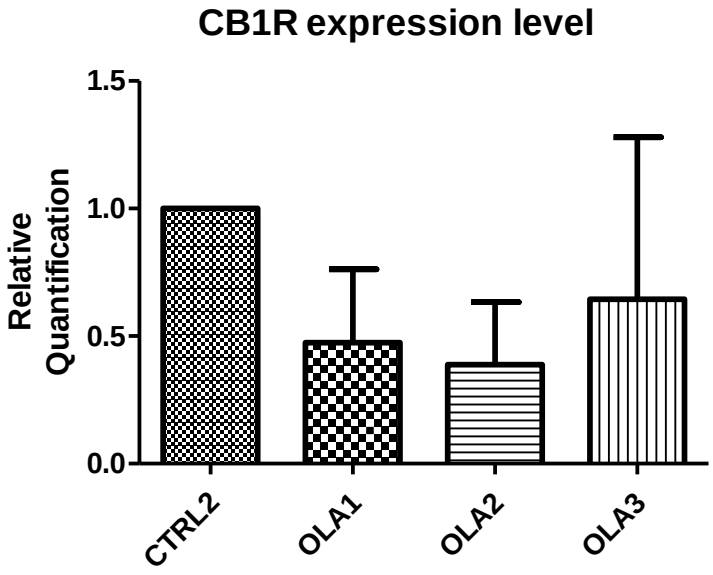

Figure 16. Fold Ct values of each group according to CTRL2´s expression. As denoted by legend from left to right; CTRL1 (light blue), OLA1 (orange), OLA2 (gray), and OLA3 (yellow).

Figure 17 described the relative quantification when OLA1 group was used as the standard for comparison. OLA1's fold Ct values, the standard for this graph, was determined at 1, OLA2's at 1,63, and OLA3's at 1,96. Again, OLA1 group, the olanzapine-only group, registered as the lowest, whereas OLA3 was listed as having the highest relative Ct value.

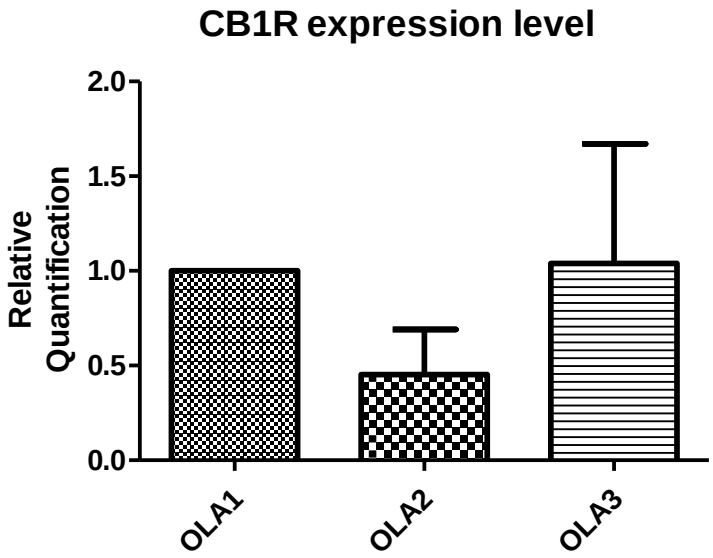

Figure 17. Fold Ct values of each group according to OLA1´s expression. As denoted by legend from left to right; OLA1 (light blue), OLA2 (orange), and OLA3 (gray).

2.17. CB1R Statistical analysis

GraphPad Prism 5 software was used. Statistical analysis was performed using One-way ANOVA accompanied with Tukey's test with. Both the control and treated groups were included for the analysis. P-value analysis was used to determine whether the difference of RT-PCR results between control and treated groups was significant enough.

One-way ANOVA's p-value analysis for statistical significance between control and treated groups was performed. P-value of the mean value comparison was detected to be less than 0.0001, which was lower than 0.05. Therefore, it could be said that there was a significant difference between the mean values of control and treated groups, and that our hypothesis that CB1R expressions in olanzapine-treated groups are higher than those in control groups was not confirmed. Table 8 showed the Tukey's multiple comparison tests between different groups, control and treated groups.

Table 8. Tukey's multiple comparison tests of CB1R mRNA's control vs affected.

Groups	Mean Diff.	q	P < 0.05?	Summary	95% CI of diff
CTRL1 vs CTRL2	0.6269	6.791	Yes	***	0.2529 to 1.001
CTRL1 vs OLA1	0.7787	8.435	Yes	***	0.4046 to 1.153
CTRL1 vs OLA2	0.6519	7.290	Yes	***	0.2896 to 1.014
CTRL1 vs OLA3	0.7057	7.645	Yes	***	0.3317 to 1.080
CTRL2 vs OLA1	0.1518	1.560	No	ns	-0.2425 to 0.5460
CTRL2 vs OLA2	0.02501	0.2645	No	ns	-0.3581 to 0.4082
CTRL2 vs OLA3	0.07883	0.8101	No	ns	-0.3154 to 0.4731
OLA1 vs OLA2	-0.1268	1.340	No	ns	-0.5099 to 0.2564
OLA1 vs OLA3	-0.07294	0.7496	No	ns	-0.4672 to 0.3213
OLA2 vs OLA3	0.05382	0.5691	No	ns	-0.3293 to 0.4370

2.18. MC3R gradient PCR analysis

To determine the appropriate MC3R annealing temperature, gradient PCR was performed. The sample used was the control group C4R2. The result was analyzed through agarose gel electrophoresis. Figure 10 showed the gradient PCR analysis on different temperatures between 57-47 degrees Celsius. The left part of the gel contained the low size DNA ladder, with range between 1000 and 50 base pairs. Our target fragment is at 123 bp, which is the area marked between 150 and 100 bp. Based on the

observation of the gel picture, the temperature 54,1 degrees Celsius seemed to be the most appropriate annealing temperature for the PCR experiment.

Figure 18. MC3R gradient PCR analyses. The left side represented DNA ladder, and both the 100 and 150 bp label indicated the specific borders closest to our intended cDNA fragment size, which is 123 bp. The columns represented the amplifications on different annealing temperatures, with the labelled temperature (54,1 ^{o}C) giving the strongest and most specific band.

2.19. MC3R standard curve

Before initiating RT-PCR, standard curve was created for fluorescence quantification. Standard curve is necessary in order to determine the relative quantification of olanzapine-treated groups when compared to the control groups. For the standard curve, control sample C4R1 of CTRL2 group was utilized as cDNA sample for RT-PCR standard reaction. In thermal cycler, the standard configuration was selected, which then measured relative quantification based on dilution level of the sample.

Figure 19 described the standard curve of MC3R quantification. For this curve, C4R1 sample was put through a series of increased dilution until the final sample's concentration was 1:10000 of the original concentration. The diluted samples were then run in thermal cycler on duplicates. After the run was over, we looked at the efficiency value to determine whether the curve is valid for use. The determination of the validity for the standard curve is based on the curve's efficiency. Standard curve's efficiency was determined to be 0,98. This value was located between 0,90 and 1,10, the acceptable range for RT-PCR standard curve. Therefore, this curve was suitable for RT-PCR analysis.

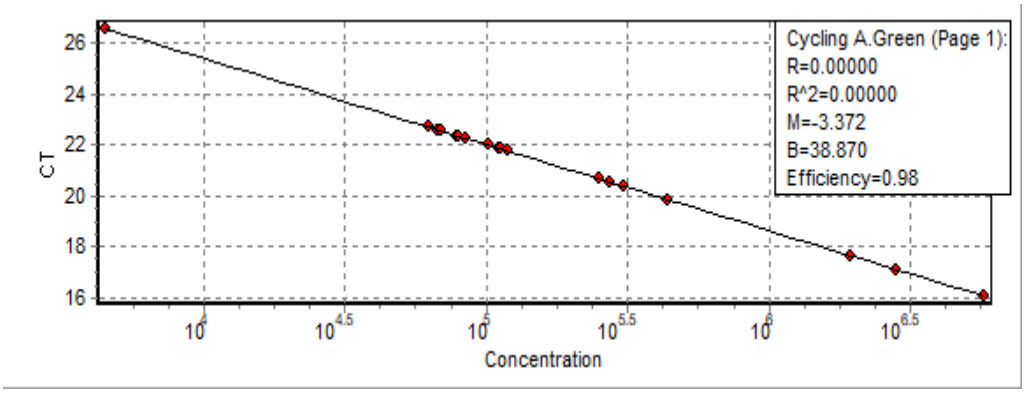

Figure 19. MC3R RT-PCR standard curve. The amplification efficiency was recorded at 0,98, which is between the acceptable range between 0,90 to 1,09 in terms of efficiency. The samples were run in duplicates, with dilutions 1/1, 1/10, 1/100, 1/1000, and 1/10000 with one copy of NTC.

2.20. MC3R RT-PCR analysis

After the relative Ct values of each group were determined, the values were listed in graphs below. Each graph had a different control used as the standard for relative Ct value comparisons. Therefore, the groups' values would change depending on the control used. Figure 20 listed the relative Ct values comparison compared to standards CTRL1, CTRL2, OLA1, and OLA1 groups.

CTRL1's fold Ct values, the standard for this graph, was at 1. While CTRL2's at 0,4, OLA1's (olanzapine-only) at 0,25, and OLA3's (olanzapine and metformin co-applied) at 0,56. The graph shows that CTRL1's value was the highest, and that the OLA1 group, the one where olanzapine was administrated solely, had the lowest value.

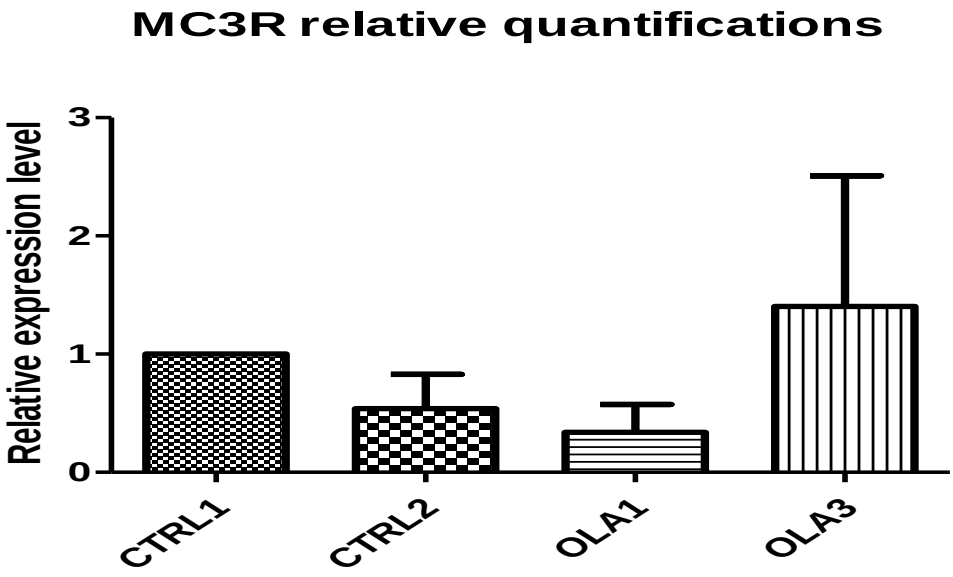

Figure 20. Fold Ct values of each groups according to CTRL1´s expression. As denoted by legend from left to right; CTRL1, CTRL2, OLA1, OLA3. Y-axis determined the relative mRNA expression levels of other groups compared to CTRL1 as the standard.

2.21. MC3R Statistical analysis

One-way ANOVA accompanied with Tukey's test was again performed for MC3R. . P-value of the mean value comparison was detected to be 0.071, which was lower than 0.05. Therefore, since p-value was lower than 0.05, it could be said that there was a significant difference between the mean values of control and treated groups, and that the hypothesis for different MC3R expressions between control and treated groups was confirmed. Table 9 gave several Tukey's multiple comparison tests between different groups.

Table 9. Tukey's multiple comparison tests of MC3R mRNA's control vs affected.

Groups	Mean Diff.	q	P < 0.05?	Summary	95% CI of diff
CTRL1 vs CTRL2	0.4610	2.250	No	ns	-0.3307 to 1.253
CTRL1 vs OLA1	0.6606	3.349	No	ns	-0.1015 to 1.423
CTRL1 vs OLA3	-0.4049	1.976	No	ns	-1.197 to 0.3869
CTRL2 vs OLA1	0.1995	0.9271	No	ns	-0.6320 to 1.031
CTRL2 vs OLA3	-0.8660	3.896	Yes	*	-1.725 to -0.007159
OLA1 vs OLA3	-1.065	4.951	Yes	**	-1.897 to -0.2340

2.22. Protein concentration analysis.

Using Bradford assay with bovine serum albumin standard, a protein standard curve was created to determine the total protein concentration. For standard curve to be valid, the standard curve's R2 value should be between the values 0.95 and 1.05. The standard curve was listed in the figure 21 below:

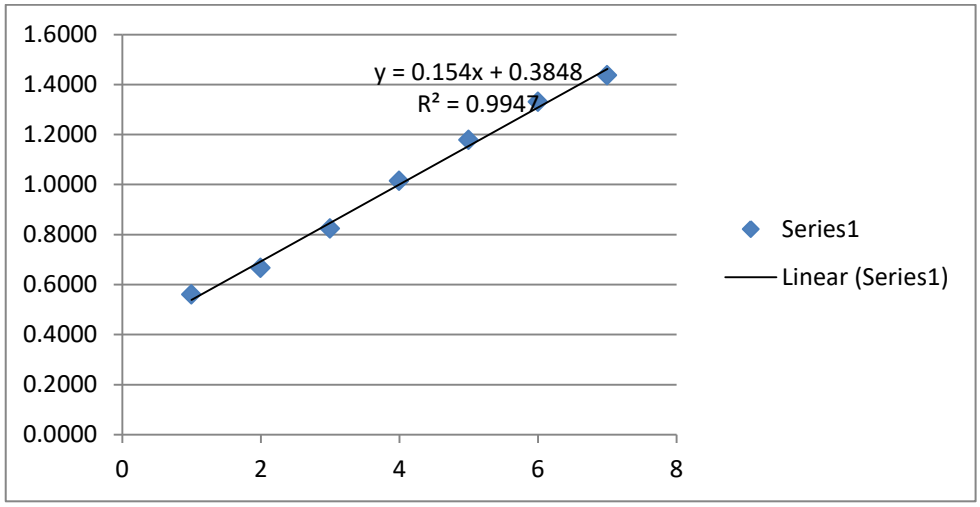

Figure 21. Protein Bradford standard curve. Y represents the light absorption value of the sample after Bradford reagent's exposure, while X represents the protein concentration. The R2 of the graph determine the curve's fidelity.

As seen in the above figure, the equation for determining protein concentration was listed as $y = 0.154x + 0.3848$, where y is the absorbance value of unknown protein and x is the concentration of said protein. Using the equation, total protein concentrations for all samples were determined.

2.23. Western blot analysis of animal groups' protein samples.

After a proper protocol had been established for the protein analyzed, all samples were run at the 10% SDS-PAGE at 75 V for approximately 3 hours. Transfers were then conducted for 20 hours at constant 30 V. After a blocking session of 20 hours in 5% BSA solution, the membranes were incubated using 1:5000 MC3R antibody solution for another 20 hours. The next day, membranes were incubated in secondary rabbit antibody solutions for 1 hour. Finally, the membranes were analyzed under the Bio-Rad UV Trans-illuminator.

Figure 22 described the western blotting results of groups CTRL1 and OLA1's four representatives. OLA1 group was administrated olanzapine from the beginning, whereas CTRL1 was not administrated any drugs. Compared to the CTRL1, we can see that the protein expression in OLA group 1 was reduced compared to CTRL1's MC3R expressions.

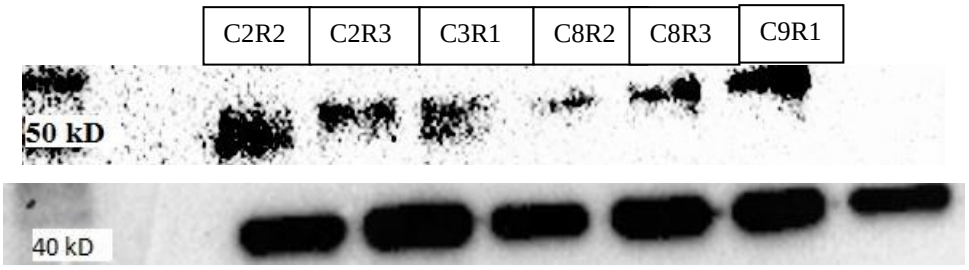

Figure 22. Western blot analysis of CTRL1 and OLA1 groups' representatives of gel 46, with GAPDH as a comparison. C2R2, C2R3, and C3R1 constituted CTRL1's group, while C8R2, C8R3, and C9R1 constituted OLA1's group. Leftmost part of the image is protein ladder where the sizes of the fragments were listed.

Figure 23 described the western blotting results of groups CTRL2 and OLA2's four representatives. Both groups were administrated metformin 7 weeks after olanzapine groups' olanzapine administration. As seen on the membrane, metformin appeared to increase MC3R's protein expression in CTRL2's group. Meanwhile, in OLA2's group the bands' expression appeared to be less apparent compared to CTRL2's group, which might be attributed through olanzapine's effect on MC3R's expression.

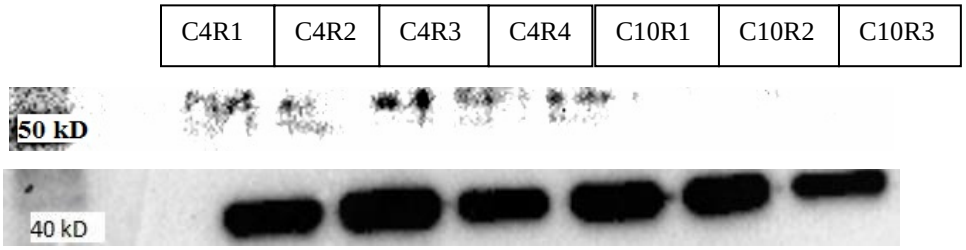

Figure 23. Western blot analysis of CTRL2 and OLA2 groups' representatives of gel 47, with GAPDH as a comparison. C4R1, C4R2, C4R3, and C4R4 constituted CTRL2's group, while C10R1, C10R2, and C10R3 constituted OLA1's group. Leftmost part of the image is protein ladder where the sizes of the fragments were listed.

Figure 24 described the western blotting results of groups OLA1, OLA2, and OLA3's representatives. OLA1's group was administered olanzapine for 14 weeks straight. OLA2's group was administered olanzapine solely for 7 weeks, and then coupled with metformin for the remaining 7 weeks. OLA3's group was co-administered both olanzapine and metformin for 14 weeks straight.

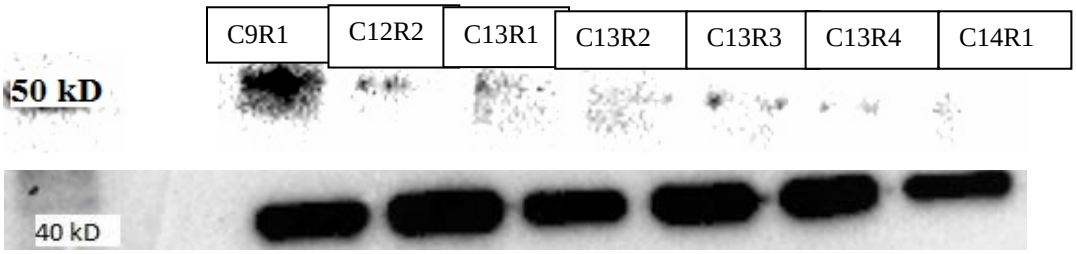

Figure 24. Western blot analysis of OLA1, OLA2, and OLA3 groups' representatives of gel 49, with GAPDH as a comparison. C9R1 constituted OLA1, while C12R2 constituted OLA2, finally C13R1 to C14R1 constituted OLA3's group,. Leftmost part of the image is protein ladder where the sizes of the fragments were listed.

Figure 25 shows the graphical comparison of relative quantification of MC3R protein expressions between each group depending on the drug treatments. CTRL1 group was not treated with any drug. Meanwhile, CTRL2 group was treated by metformin from the seventh up to the fourteenth week. OLA1 group was administered olanzapine for the whole 14 weeks. OLA2 group was initially only administered olanzapine for 7 weeks, then for the remaining seven weeks the group was co-administered both olanzapine and metformin. Finally, OLA3 group was co-administered both olanzapine and metformin for 14 weeks.

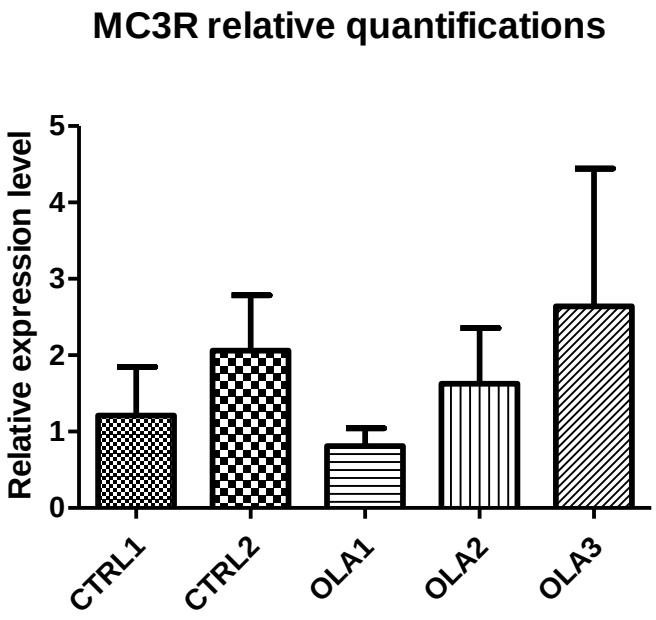

Figure 25. MC3R relative protein expression graph. X-axis represented the groups analyzed, where Y-axis represented the relative expression levels of the protein.

One-way ANOVA accompanied with Tukey's test was again performed for MC3R protein analysis.. P-value of the mean value comparison was detected to be 0.0279, which was lower than 0.05. Therefore, since p-value was lower than 0.05, it could be said that there was a significant difference between the mean values of control and

treated groups, and that the hypothesis for different MC3R expressions between control and treated groups was confirmed. Table 10 below described Tukey's multiple comparison tests between each group of rats.

Table 10. Tukey's multiple comparison tests of MC3R protein's expressions between control vs affected.

Groups	Mean Diff.	q	P < 0.05?	Summary	95% CI of diff
CTRL1 vs CTRL2	-0.8468	1.795	No	ns	-2.787 to 1.093
CTRL1 vs OLA1	0.4013	0.8706	No	ns	-1.494 to 2.297
CTRL1 vs OLA2	-0.4138	0.8977	No	ns	-2.309 to 1.482
CTRL1 vs OLA3	-1.428	3.026	No	ns	-3.368 to 0.5126
CTRL2 vs OLA1	1.248	3.204	No	ns	-0.3539 to 2.850
CTRL2 vs OLA2	0.4330	1.112	No	ns	-1.169 to 2.035
CTRL2 vs OLA3	-0.5807	1.444	No	ns	-2.235 to 1.074
OLA1 vs OLA2	-0.8150	2.166	No	ns	-2.363 to 0.7326
OLA1 vs OLA3	-1.829	4.695	Yes	*	-3.431 to -0.2268
OLA2 vs OLA3	-1.014	2.603	No	ns	-2.616 to 0.5882

CHAPTER 4

DISCUSSSION

Previously the effects of olanzapine with/without metformin coupling on the expressions of neurohormones NPY and POMC, which are two of the most important weight regulators of the hypothalamus's the ARC region, was investigated in several previous projects of our laboratory. The aim of this project was to investigate the effects of olanzapine from a different point of view; the expressions of CB1R and MC3R in male Wistar rats, the two receptors known to regulate energy and lipid metabolism, respectively.

Endocannabinoid system, by which CB1R is the part of, has been heavily investigated as a crucial part in energy metabolism. In an experiment to investigate obesity as a phenotypic side effect of Prader-Willi Syndrome, both gene and protein expression levels of CB1R were significantly upregulated (Knani et al., 2016). MC3R dysregulation, however, has not been thoroughly investigated in its role to obesity phenotype formation. One experiment determined that MC3R was required for food anticipatory response (FAA) behavior management in mice models (Girardet et al., 2014).

Due to the increases of body weights of olanzapine-administered rats detected in the previous experiment conducted by one of our laboratory's students, the increases in CB1R mRNA and decreases in MC3R mRNA's expressions were hypothesized. However, a decrease in CB1R mRNA expressions of groups where olanzapine was

administered without metformin was detected instead. Furthermore, metformin did not cause a significant improvement to the CB1R expression. In a previous experiment, a CB1R antagonist deployed managed to decrease both CB1R mRNA's expression in both liver and white adipose tissues, accompanied by decreased weight and increased insulin sensitivity (Tang et al., 2012). Results from other publications (Kabir et al., 2015, Osei-Hyaman et al., 2005) also supported these observations.

Given the effects of olanzapine on CB1R had already been researched in terms of binding density aspect (Weston-Green et al, 2012), we attempted to determine olanzapine's impact on its expression in ARC nucleus region of hypothalamus. Results of our experiment seemed to convey that olanzapine had no effect on CB1R's gene expression, but instead it might have other impact on CB1R's functions such as intracellular pathways governed by it, and that more research would be required in order to elucidate the thorough mechanism of olanzapine on ECS' functions.

Meanwhile, results of MC3R's gene expression in terms of DNA fragment (with RT-PCR) and protein (with western blot) yielded expected results, with olanzapine-only group (OLA1) having the lowest expression levels on both gene and protein samples. From the previous research of our lab (Kurt, 2014), the levels of POMC expression were determined to be lower in olanzapine-administered animals. In this research, the levels of gene expressions of MC3R seemed to reveal that olanzapine also lowered the protein level of MC3R, which might lead to olanzapine-treated groups having higher adipose tissue formations compared to control groups.

As for metformin's effect on MC3R expression on olanzapine-administered rats, MC3R's expression was shown to increase in olanzapine and metformin-administered groups compared to solely olanzapine-administered groups. In control groups, metformin-administered group (CTRL2) also showed MC3R's protein expression increase compared to non-administered group (CTRL1). This observation gave some insight on how metformin alleviate olanzapine-induced weight gain on rats. Through increasing MC3R's expression, the feeding rate might be decreased and subsequently decreased weight gain.

Given that there were few researches on the antipsychotics' effects on both endocannabinoid and melanocortin system's receptor expressions, not many journals and references which could prove our hypotheses had been published. One of the most relevant researches investigated the effects of amphetamine on expression levels of NPY, POMC, and MC3R proteins. Coinciding with the decreased weight and feeding rate, a marked increase in MC3R's expression was detected (Kuo et al., 2012).

Lack of research on MC3R also gave impact on the availability of primary antibodies for MC3R in the market. Our primary antibody was purchased from Santa Cruz (Santa Cruz Biotechnology, Dallas, Texas, USA). Although the antibody itself was recommended, we weren't able to get a satisfying blot picture after numerous attempts of optimization. Unfortunately, as of this moment the product had been discontinued. Another aspect that affected our experiment was the scarcity of the animal materials at hand, given the leftover of both hypothalamic total RNA and protein samples were not plentiful due to being utilized by previous experiments.

CHAPTER 5

CONCLUSIONS

- In our experiment, CB1R mRNA's expression's increase was not observed in olanzapine-administered groups compared to control groups. Furthermore, metformin seemed to have no noticeable contribution in decreasing the CB1R gene expresions in both OLA2 and OLA3 groups This contradicted the hypothesis formulated that CB1R's gene expression would be increased after olanzapine's administration for a considerable period of time, and metformin would counteract this rise in gene expression. CB1R was detected to have increased expression in obese patients (Trillou et al, 2003; Hildebrant et al, 2003). This observation suggested that olanzapine worked on an alternative pathway in order to induce weight gain in male Wistar rats.
- Meanwhile, MC3R mRNA's expression's slight decrease was observed in olanzapine-administered groups compared to control groups. Another observation revealed that metformin seemed to cause increases in MC3R's gene expression. This went in the line with the hypothesis formulated that MC3R's gene expression would decrease after olanzapine administration. MC3R deficiency was known to be affecting weight gain and especially fat disposition by increasing lipid mass and reducing lean mass (Chen et al, 2000). This observation might give us a clue in how antipsychotics interfere with energy metabolism of patients' body.
- Protein analysis through western blotting revealed a behavior mirroring aforementioned gene expression comparison between olanzapine-treated and

control groups. Metformin was observed to be increasing MC3R protein expressions, and that the longer duration of treatment managed to further increase the protein expression observed. MC3R was known to be responsible in the management of adipose tissue (Renquist et al, 2012). Given that the previous experiment (Kurt, 2014) revealed a high expression of adipose tissue in olanzapine-treated groups, this observation seemed to determine that olanzapine might cause weight gain through MC3R manipulation.

- From the experiment, MC3R could be seen as one of the factors in olanzapine-induced obesity. However, given that there were few publications regarding the effects of antipsychotics on the MC3R's expressions and mechanisms, further research would be required to determine whether olanzapine works directly or indirectly on the receptor.

REFERENCES

1. Leucht et al. 2009. *Second-generation versus first-generation antipsychotic drugs for schizophrenia: a meta-analysis*. The Lancet, Volume 373, Issue 9657, 3-9 January 2009, pages 31-41.

2. ÜÇOK, A, Gaebel, W., 2008. *Side effects of atypical antipsychotics: a brief overview*. World Psychiatry, 2008 Feb 7 (1), 58-62.

3. Bymaster et al., 1997. *In vitro and in vivo biochemistry of Olanzapine: a novel, atypical antipsychotic drug*. Journal of Clinical Psychiatry, 1997; 58(Supplement 10): 28-36.

4. de Leon et al., 2005. *The Dosing of Atypical Antipsychotics.* Psychosomatics, Volume 46, Issue 3, May-June 2005, Pages 262-273.

5. Tohen et al., 1999. *Olanzapine versus placebo in the treatment of acute mania. Olanzapine HGEH study group.* Am J Psychiatry. 1999 May; 156(5); 702-9.

6. Tohen, Baker et al., 2002. *Olanzapine versus divalproex in the treatment of acute mania.* American Journal of Psychiatry. 2002;159:1011–17.

7. Zajecka et al., 2002. *A comparison of the efficacy, safety, and tolerability of divalproex sodium and olanzapine in the treatment of bipolar disorder*. The journal of Clinical Psychiatry, 2002; 1148-1155.

8. Tohen, Vieta et al., 2003. *Efficacy of olanzapine and olanzapine-fluoxetine combination in the treatment of bipolar I depression*. Archives of General Psychiatry. 2003;60:1079–88.

9. Brown EB, McElroy SL, Keck PE, Jr, et al., 2006. *A 7-week, randomized, double-blind trial of olanzapine/fluoxetine combination versus lamotrigine in the treatment of bipolar I depression*. Journal of Clinical Psychiatry. 2006;67:1025–33.

10. Haddad, P., 2005. *Weight change with atypical antipsychotics in the treatment of schizophrenia*. Journal of Psychopharmacology. **2005** Nov;19(6 Suppl):16-27.

11. Dong et al. 2015. *A2BP1 gene polymorphisms association with olanzapine-induced weight gain.* Pharmacological Research, Volume 99, September 2015, Pages 155–161

12. Wani et al., 2015. *Effects of switching from olanzapine to aripiprazole on the metabolic profiles of patients with schizophrenia and metabolic syndrome: a double-blind, randomized, open-label study*. Neuropsychiatric Disease and Treatment, 2015; 11: 685–693.

13. Cota, D., 2007. *CB1 receptors: emerging evidence for central and peripheral mechanisms that regulate energy balance, metabolism, and cardiovascular health.* Diabetes/Metabolism Research and Reviews, Volume 23, Issue 7, pages 507–517, October 2007.

14. Brown et al., 1977. *Kinetic studies of food intake and sucrose solution preference by rats treated with low doses of delta9-tetrahydrocannabinol*. *Behav Biol* 1977; **20**: 104–110.

15. Hao et al., 2000. *Low dose anandamide affects food intake, cognitive function, neurotransmitter and corticosterone levels in diet-restricted mice*. *Euro J Pharmacology* 2000; **392**: 147–156.

16. Cota et al., 2003. *The endogenous cannabinoid system affects energy balance via central orexigenic drive and peripheral lipogenesis*. *Journal of Clinical Investigation* 2003; **112**: 423–431.

17. Gardner EL., 2005. *Endocannabinoid signaling system and brain reward: emphasis on dopamine*. *Pharmacol Biochem Behav* 2005; **81**:263–284.

18. Williams CM, Kirkham TC., 2002. *Observational analysis of feeding induced by Delta9-THC and anandamide*. *Physiology and Behavior* 2002; **76**:241–250.

19. Ravinet Trillou C, et al (2003). *Anti-obesity effect of SR141 716, a CB1 receptor antagonist, in diet-induced obese mice*. *American Journal of Physiology: Regulatory, Integrative and Comparative Physiology* 2003; **284**: R345–R353.

20. Engeli S, et al (2005). *Activation of the peripheral endocannabinoid system in human obesity*. *Diabetes* 2005;**54**: 2838–2843.

21. Bluher M, et al (2006). *Dysregulation of the peripheral and adipose tissue endocannabinoid system in human abdominal obesity*. *Diabetes* 2006; **55**: 3053–3060.

22. Di S, et al (2003). *Nongenomic glucocorticoid inhibition via endocannabinoid release in the hypothalamus: a fast feedback mechanism*. *Journal of Neuroscience* 2003; **23**: 4850–4857.

23. Berger A, et al (2001). *Anandamide and diet: inclusion of dietary arachidonate and docosahexaenoate leads to increased brain levels of the corresponding N-acylethanolamines in piglets. Proc Natl Acad Sci U S A* 2001; **98**: 6402–6406.

24. Sipe J, et al (2005) *Overweight and obesity associated with a missense polymorphism in fatty acid amide hydrolase (FAAH). Int J Obes Relat Metab Disord* 2005; **29**: 755–759.

25. Siegfried Z, et al (2004). *Association study of cannabinoid receptor gene (CNR1) alleles and anorexia nervosa: differences between restricting and binging/purging subtypes. Am J Med Genet B Neuropsychiatr Genet* 2004; **125**: 126–130.

26. Mailleux P, et al (1992). *Distribution of cannabinoid receptor messenger RNA in the human brain: an in situ hybridization histochemistry with oligonucleotides. Neurosci Lett* 1992; **143**: 200–204.

27. Herkenham M, et al (1991). *Characterization and localization of cannabinoid receptors in rat brain: a quantitative in vitro autoradiographic study. J Neurosci* 1991; **11**: 563–583.

28. Breivogel CS, Childers SR (1998). *The functional neuroanatomy of brain cannabinoid receptors. Neurobiol Dis* 1998; **5**: 417–431.

29. Howlett AC, et al (2002). *International Union of Pharmacology. XXVII. Classification of cannabinoid receptors. Pharmacol Rev* 2002; **54**: 161–202.

30. McAllister SD, et al (1999). *Cannabinoid receptors can activate and inhibit G protein-coupled inwardly rectifying potassium channels in a Xenopus oocyte expression system. J Pharmacol Exp Ther*291:618–626.

31. Gebremedhin D, et al (1999). *Cannabinoid CB1 receptor of cat cerebral arterial muscle functions to inhibit L-type Ca^{2+} channel current*. *Am J Physiol* 276:H2085–H2093.

32. Pan X, et al (1996) *Rat brain cannabinoid receptor modulates N-type Ca^{2+} channels in a neuronal expression system*. *Mol Pharmacol* 49:707–714.

33. Mackie K, et al (1995*). Cannabinoids activate an inwardly rectifying potassium conductance and inhibit Q-type calcium currents in AtT20 cells transfected with rat brain cannabinoid receptor. J Neurosci* 15:6552–6561.

34. Hampson AJ, et al (1998) *Dual effects of anandamide on NMDA receptor-mediated responses and neurotransmission. J Neurochem*70:671–676.

35. Sugiura T, et al (1996) *2-Arachidonoylglycerol, a putative endogenous cannabinoid receptor ligand, induces rapid, transient elevation of intracellular free Ca^{2+} in neuroblastoma x glioma hybrid NG108-15 cells*. *Biochem Biophys Res Commun* 229:58–64.

36. Derkinderen P, et al (1996) *Regulation of a neuronal form of focal adhesion kinase by anandamide*. *Science (Wash DC)* 273:1719–1722.

37. Wartmann M, et al (1995) *The MAP kinase signal transduction pathway is activated by the endogenous cannabinoid anandamide*. *FEBS Lett* 359:133–136.

38. Gómez del Pulgar., T, et al (2000) *The CB_1 cannabinoid receptor is coupled to the activation of protein kinase B/Akt*. *Biochem J*347:369–373

39. Sánchez C., et al (2001) *The CB_1 cannabinoid receptor of astrocytes is coupled to sphingomyelin hydrolysis through the adaptor protein Fan*. *Mol Pharmacol* 59:955–959.

40. Van Gaal LF, et al (2005) *Effects of the cannabinoid-1 receptor blocker rimonabant on weight reduction and cardiovascular risk factors in overweight patients: 1-year experience from the RIO-Europe study*. *Lancet* 2005; **365**:1389–1397.

41. Scheen AJ, et al (et al). *Efficacy and tolerability of rimonabant in overweight or obese patients with type 2 diabetes: a randomised controlled study*. *Lancet* 2006; **368**: 1660–1672.

42. Poirier B, et al (2005). *The anti-obesity effect of rimonabant is associated with an improved serum lipid profile*. *Diabetes Obes Metab* 2005; **7**: 65–72.

43. Despres JP, et al (2005) *Effects of rimonabant on metabolic risk factors in overweight patients with dyslipidemia*. *N Engl J Med* 2005; **353**: 2121–2134.

44. Pi-Sunyer FX, et al (2006) *Effect of rimonabant, a cannabinoid-1 receptor blocker, on weight and cardiometabolic risk factors in overweight or obese patients: RIO-North America: a randomized controlled trial*. *JAMA* 2006;**295**: 761–775.

45. Weston-Green et al (2012). *Alterations to Melanocortinergic, GABAergic and Cannabinoid Neurotransmission Associated with Olanzapine-Induced Weight Gain.* PLoS One. 2012; 7(3): e33548.

46. Park et al (2011). *Cannabinoid type 1 receptor gene polymorphisms are not associated with olanzapine-induced weight gain*. Human Psychopharmacology: Clinical and Experimental Volume 26, Issue 4-5, pages 332–337, June/July 2011

47. Pandit et al (2016). *Melanocortin 3 Receptor Signaling in Midbrain Dopamine Neurons Increases the Motivation for Food Reward.* Neuropsychopharmacology. 2016 Aug; 41(9): 2241–2251.

48. Grieco et al (2000). *D-Amino acid scan of gamma-melanocyte-stimulating hormone: importance of Trp(8) on human MC3 receptor selectivity*. Journal of Medical Chemistry 2000, Dec 28; 43 (26): 4998-5002.

49. Joseph et al (2010). *γ_2-Melanocyte stimulation hormone (γ_2-MSH) truncation studies results in the cautionary note that γ_2-MSH is not selective for the mouse MC3R over the mouse MC5R.* Peptides, Volume 31, Issue 12, December 2010, Pages 2304–2313.

50. Knani et al (2016). *Targeting the endocannabinoid/CB1 receptor system for treating obesity in Prader-Willi syndrome*. MOLECULAR METABOLISM 5 (2016) 1187-1199.

51. Renquist et al. (2012). *Melanocortin-3 receptor regulates the normal fasting response*. Proc Natl Acad Sci U S A. 2012 Jun 5; 109(23): E1489–E1498.

52. Sutton et al. (2008). *The melanocortin-3 receptor is required for entrainment to meal intake.* J Neurosci. 2008 Nov 26; 28(48): 12946–12955.

53. Chen et al. (2000). *Inactivation of the mouse melanocortin-3 receptor results in increased fat mass and reduced lean body mass*. *Nature Genetics* **26**, 97 - 102 (2000).

54. Mavrikaki et al. (2016). *Melanocortin-3 receptors in the limbic system mediate feeding-related motivational responses during weight loss*. Mol Metab. 2016 Jul; 5(7): 566–579.

55. Diamanti-Kandarakis et al. (2010). *Metformin: an old medication of new fashion: evolving new molecular mechanisms and clinical implications in polycystic ovary syndrome*. European Journal of Endocrinology (2010) 162 193–212.

56. Gao et al. (2013). *Effect of combined treatment with clozapine and metformin on fasting blood glucose, insulin level, and expression of the glucose transporter-2 ($GLUT_2$) in Sprague-Dewey Rats*. Shanghai Archives of Psychiatry, 2013, Vol. 25, No. 3.

57. Remington et al. (2015). *Metformin attenuates olanzapine induced hepatic, but not peripheral insulin resistance*. Journal of Endocrinology (2015) 227, 71–81.

58. Girardet et al. (2014). *Assessing Interactions Between Ghsr and Mc3r Reveals a Role for AgRP in the Expression of Food Anticipatory Activity in Male Mice*. Endocrinology. 2014 Dec; 155(12): 4843–4855.

59. Tang et al. (2012). *Beneficial Metabolic Effects of CB1R Anti-Sense Oligonucleotide Treatment in Diet-Induced Obese AKR/J Mice.* PLoS ONE. August 2012 | Volume 7 | Issue 8.

60. |Kabir et al. (2015). *CB1R antagonist increases hepatic insulin clearance in fat-fed dogs likely via upregulation of liver adiponectin receptors.* Am J Physiol Endocrinol Metab. 2015 Oct 15; 309(8): E747–E758.

61. Osei-Hyaman et al. (2005). *Endocannabinoid activation at hepatic CB1 receptors stimulates fatty acid synthesis and contributes to diet-induced obesity.* The Journal of Clinical Investigation.Volume 115 Number 5 May 2005.

62. Miksys et al. (2017). *Rat brain CYP2D enzymatic metabolism alters acute and chronic haloperidol side-effects by different mechanisms*. Progress in Neuro-Psychopharmacology and Biological Psychiatry. Available online 26 April 2017.

63. Haslam, D.W., James, P.T. (2005). *Obesity.* The Lancet, Volume 366, Issue 9492, 1–7 October 2005, Pages 1197–1209.

64. Boswell, T., Dunn, I.C. (2017) *Regulation of Agouti-Related Protein and Pro-Opiomelanocortin Gene Expression in the Avian Arcuate Nucleus.* Front Endocrinol (Lausanne). 2017; 8: 75.

65. Bressington et al. (2016). *Cardiometabolic health, prescribed antipsychotics and health-related quality of life in people with schizophrenia-spectrum disorders: a cross-sectional study*. BMC Psychiatry (2016) 16:411.

66. Panariello et al (2012). *The Role of Leptin in Antipsychotic-Induced Weight Gain: Genetic and Non-Genetic Factors.* Journal of Obesity Volume 2012, Article ID 572848, 7

67. Li et al. (2016). *Chronic Olanzapine Treatment Induces Disorders of Plasma Fatty Acid Profile in Balb/c Mice: A Potential Mechanism for Olanzapine-Induced*

Insulin Resistance. PLOSONE | DOI:10.1371/journal.pone.0167930 December 14, 2016

68. Suvitaival et al. (2016). *Serum metabolite profile associates with the development of metabolic co-morbidities in first-episode psychosis*. Translational Psychiatry (2016) 6,e951; doi:10.1038/tp.2016.222; published online 15 November 2016.

69. Morozov et al. (2017). *Cannabinoid type 1 receptor-containing axons innervate NPY/AgRP neurons in the mouse arcuate nucleus.* MOLECULAR METABOLISM 6 (2017) 374-381.

70. Chen, B. and Hu., N. (2017). *Rimonabant improves metabolic parameters partially attributed to restoration of high voltage-activated Ca2+channels in skeletal muscle in HFD-fed mice.* Brazilian Journal of Medical and Biological Research (2017) 50(6): e6141, http://dx.doi.org/10.1590/1414-431X20176141.

71. Baeza et al. (2017). *The effects of antipsychotics on weight gain, weight-related hormones and homocysteine in children and adolescents: a 1-year follow-up study.* Eur Child Adolesc Psychiatry (2017) 26:35–46.

72. Newcomer J. (2005). *Second-generation (atypical) antipsychotics and metabolic effects: a comprehensive literature review*. CNS Drugs. 2005, 19 Suppl 1:1-93.

73. Olanzapine-olanzapine tablet, film-coated by Mylan Pharmaceutical. Retrieved from https://www.dailymed.nlm.nih.gov/dailymed/archives/fdaDrugInfo.cfm?archiveid=171848 at June 13th, 2017.

74. Busquest-Garcia et al (2015). *Dissecting the cannabinergic control of behavior: The where matters*. Bioessays 37: 0000–0000,_ 2015 WILEY Periodicals, Inc.

75. *Diabetes Drug Metformin Could Help You Live Longer.* Biohealthscience (BHS) article written on July30, 2013. Retrieved from http://www.biohealthscience.com/2013/07/diabetes-drug-metformin-could-help-you-live-longer/.

76. Bak et al. (2014). *Almost All Antipsychotics Result in Weight Gain: A Meta-Analysis*. PLOS ONE | www.plosone.org-1-April 2014 | Volume 9 | Issue 4 | e94112.

77. Boon et al. (2014). *Peripheral cannabinoid 1 receptor blockade activates brown adipose tissue and diminishes dyslipidemia and obesity*. The FASEB Journal article fj.13-247643. Published online August 25, 2014.

78. Plum et al. (2017). *Central insulin action in energy and glucose homeostasis.* The Journal of Clinical Investigation. Volume 116, Number 7.

79. Lian et al. (2014). *Preventing Olanzapine-Induced Weight Gain Using Betahistine: A Study in a Rat Model with Chronic Olanzapine Treatment.* PLOS ONE | www.plosone.org. August 2014 | Volume 9 | Issue 8 | e104160.

80. Kursungoz et al. (2015). *Effects of risperidone treatment on the expression of hypothalamic neuropeptide in appetite regulation in Wistar rats.* Brain Research. Volume 1596, 30 January 2015, Pages 146–155.

81. Rodrigues et al (2014). *Intracellular signaling mechanisms of the melanocortin receptors: Current state of the art.* Cellular and Molecular Life Sciences CMLS · December 2014.

82. Mahmood, T., and Yang, P. (2012). *Western Blot: Technique, Theory, and Trouble Shooting*. N Am J Med Sci. 2012 Sep; 4(9): 429–434.

83. Kuo et al. (2012). *Involvement of neuropeptide Y Y1 receptor in the regulation of amphetamine-mediated appetite suppression.* Neuropharmacology, Volume 63, Issue 5, October 2012, Pages 842–850.

84. Rojo et al. (2015). *ReviewMetabolic syndrome and obesity among users of second generationantipsychotics: A global challenge for modern psychopharmacology.* Pharmacol Res (2015), http://dx.doi.org/10.1016/j.phrs.2015.07.022.

85. Ak et al. (2013). *The investigation of leptin and hypothalamic neuropeptides role in first attack psychotic male patients: Olanzapine monotherapy.* Psychoneuroendocrinology (2013) 38, 341—347.

86. Yanik et al. (2013). *Weight Gain in Risperidone Therapy*. J Clin Psychopharmacol 2013;33: 608Y613.

87. Breum, L. and Fernstorm, M.H. (2001). *International Textbook of Obesity.* Chichester, UK: John Wiley & Sons, Ltd.

88. Kang et al. (2017). *Activation of the ATF2/CREB-PGC-1α pathway by metformin leads to dopaminergic neuroprotection.* Oncotarget, Advance Publications 2017.

89. Sezlev-Bilecen et al. (2016). *Dysregulation of hypothalamic modulation in olanzapine treated male rats.* Progress in Neuro-Psychopharmacology & Biological Psychiatry 71 (2016) 103–107.

90. Barsh, G.S. and Schwartz, M.W. (2002). *GENETIC APPROACHES TO STUDYING ENERGY BALANCE: PERCEPTION AND INTEGRATION*. NATURE REVIEWS | GENETICS VOLUME 3 | AUGUST 2002 | 589.

91. Simoes et al (2013). *Efficient recovery of proteins from multiple source samples after trizol® or trizol®LS RNA extraction and long-term storage.* Simõeset al. BMC Genomics 2013,14:181.

APPENDIX A

RNA CONCENTRATIONS OF EVERY ANIMAL IN EVERY GROUP

Table A. 1. Total animals' hypothalamic RNA samples.

Animals	Concentration (ng/µL)	A260/230	A260/280
C1R1	1032	2.071	1.968
C1R2	368.8	2.077	2.058
C1R3	967.2	2.099	2.046
C1R4	738.4	2.011	2.07
C2R1	1181.2	2.14	1.98
C2R2	900	2.091	2.09
C2R3	733.6	2.038	2.094
C3R1	715.2	1.886	2.094
C3R2	916.8	2.076	2.091
C3R3	860.8	2.053	2.085
C4R1	501.6	2.056	2.14
C4R2	962.4	2.022	2.152
C4R3	543.2	1.64	2.156
C4R4	604.8	2.061	2.149
C5R1	481.6	1.887	2.173
C5R2	620.8	2.18	2.138
C5R3	1082.4	2.127	2.161
C6R1	863.8	2.132	2.136
C6R2	408.8	1.907	2.112
C6R3	456.8	2.123	2.137
C7R1	471.2	1.957	2.096

Table A.1. (Continued)

C7R2	493.6	1.946	2.15
C7R3	590.4	2.067	2.145
C7R4	511.2	2.109	2.144
C8R1	693.6	2.12	2.135
C8R2	820.8	2.174	2.133
C8R3	684.8	2.088	2.14
C9R1	1203.2	2.115	2.149
C9R2	459.2	2.158	2.126
C9R3	816.8	2.14	2.14
C10R1	768.8	2.164	2.145
C10R2	755.2	2.18	2.136
C10R3	460.8	2.525	2.133
C10R4	1020	1.596	2.073
C11R1	492	1.984	2.15
C11R2	730.4	2.052	2.143
C11R3	750.4	2.089	2.146
C12R1	530.4	1.802	2.091
C12R2	856.8	2.052	2.155
C12R3	515.2	2.098	2.118
C13R1	740	1.919	2.156
C13R2	524	1.997	2.12
C13R3	532	2.052	2.111
C13R4	316	1.975	2.112
C14R1	668.8	2.029	2.155
C14R2	1227.2	2.148	2.148
C14R3	516.8	2.091	2.118
C15R1	1037.6	2.173	2.147
C15R2	539.2	1.872	2.093
C15R3	1234.4	2.114	2.158

APPENDIX B

MC3R WESTERN BLOT PROCEDURE

B. 1 Samples were mixed with 4x protein loading dye which will denature the proteins inside that it could be separated based on the primary amino acid sequences.

B. 2 Samples were then heated using heating arrangements as follows: 5 minutes initial heating at 50^{o}C, 20 minutes of heating at 95 ^{o}C, and 5 minutes at 40 ^{o}C.

B. 3 Load 1 X running buffer into the gel apparatus after assembling the gels inside. Samples were loaded in the wells of SDS-PAGE gels using micropipettes.

B. 4 SDS-PAGE gels were then run at 75 V until the protein ladder has been established.

B. 5 Meanwhile, PVDF membranes were cut at the dimension of 8 x 6 cm. Prepare two membranes for two gels. Both membranes were immersed in methanol for 15 seconds, distilled water for 2 minutes, and then 1X transfer buffer for 15 minutes along with transfer apparatuses.

B. 6 After running, gels were immersed in 1X transfer buffer for 15 minutes.

B. 7 The transfer sandwich was prepared:

a. Open the container and put a black sponge on the black side of the container.
b. Put one piece of Whatman paper on top of the black sponge.
c. Put the gel on the Whatman paper.

d. Put the membrane on top of the gel and remove all air bubbles using a roller.
e. Put another piece of Whatman paper on top of the membrane and then another black sponge on top of the paper.
f. Lock the sandwich and make sure that both gel and membrane are not dehydrated.

B.8 The transfer apparatus was assembled, and then drenched with 1X transfer buffer inside the transfer container. The transfer was run at 30 V overnight.

B.9 Blocking solution was prepared as 5% BSA, 0.1% T-TBS. Both membranes were drenched in blocking solution overnight.

B.10 After blocking, the blocking solution was discarded and the membranes were washed with 0.1% T-TBS for 5 times at 5 minutes each.

B.11 Primary antibody solution was prepared as 5% BSA, 0.1% T-TBS with appropriate concentrations, and then both membranes were incubated overnight at 4 degrees Celsius.

B.12 Primary antibody solution was discarded, and then both membranes were washed another 5 times for 5 minutes each with T-TBS buffer.

B.13 Secondary antibody solution was prepared as 5% BSA, 0.1% T-TBS with appropriate concentrations, and then both membranes were incubated for 1 hour at room temperature.

B.14 Secondary antibody solution was discarded, and then both membranes were washed with T-TBS for 10 minutes twice and then with TBS for 10 minutes once.

B.15 ECL clarity solution was prepared as 1:1 ratio. Both membranes were covered with the mixtures in the dark for 1 minute, and then the membranes were visualized using UV transilluminator for 100 seconds for the picture.

APPENDIX C

TABLES OF ANIMAL GROUPS AND MATERIALS

Table C. 1. List of both control and treated animals' RNA samples.

CTRL1	CTRL2	OLA1	OLA2	OLA3
C1R1	C4R1	C7R1	C10R1	C13R1
C1R2	C4R2	C7R2	C10R2	C13R2
C1R3	C4R3	C7R3	C10R3	C13R3
C1R4	C4R4	C7R4	C10R4	C13R4
C2R1	C5R1	C8R1	C11R1	C14R1
C2R2	C5R2	C8R2	C11R2	C14R2
C2R3	C5R3	C8R3	C11R3	C14R3
C3R1	C6R1	C9R1	C12R1	C15R1
C3R2	C6R2	C9R2	C12R2	C15R2
C3R3	C6R3	C9R3	C12R3	C15R3

Table C. 2. Gene's primer sequences.

Name	Sequences
CB1R: Forward	5′ACAGCCAGCATGCACAGGGC
CB1R: Reverse	5′CGGCGGACGTGTCTGTGGAC
MC3R: Forward	5′AAGCCCTCTCCTTGATCGTG
MC3R: Reverse	5′AGCACCATGGCGAAGAACAT

Table C. 3. cDNA synthesis reagents.

Materials (1st phase)	Amounts
mRNA amount (500 nM)	Adjustable according to mRNA concentrations.
Random Hexamer Primer	1 µL
NFW	Adjustable according to mRNA concentrations.
Total	12 µL
Materials (2nd phase)	**Amounts**
5x Reaction Buffer	4 µL
10 mM dNTP Mix	2 µL
RiboLock RNAse inhibitor	1 µL
RevertAid Reverse Transcriptase	1 µL
Total	20 µL

Table C. 4. CB1R and MC3R gradient PCR reagents.

Reagents	Volume/ PCR tubes
10x PCR Buffer	5 µL
10 mM dNTP Mix	1 µL
Forward primers (4 µM concentration)	1 µL
Reverse primers (4 µM concentration)	1 µL
25 mM $MgCl_2$ (1,5 mM final concentration)	2,4 µL
CDNA (0,5 µM)	1 µL
Taq polymerase	0,25 µL
NFW	8,35 µL
Total	20 µL

Table C. 5. List of both control and treated animals' protein samples.

CTRL1	CTRL2	OLA1	OLA2	OLA3
C1R1	C4R1	C7R1	C10R1	C13R1
C1R2	C4R2	C7R2	C10R2	C13R2
C1R3	C4R3	C7R3	C10R3	C13R3
C1R4	C4R4	C7R4	C10R4	C13R4
C2R1	C5R1	C8R1	C11R1	C14R1
C2R2	C5R2	C8R2	C11R2	C14R2
C2R3	C5R3	C8R3	C11R3	C14R3
C3R1	C6R1	C9R1	C12R1	C15R1
C3R2	C6R2	C9R2	C12R2	C15R2
C3R3	C6R3	C9R3	C12R3	C15R3

Table C. 6. Separating and stacking gel's materials.

10% separating gel	2 gels vol.	4% stacking gel	2 gels vol.
Distilled water	6 mL	Distilled water	3 mL
30% Acrylamide/Bis-Acrylamide	5 mL	30% Acrylamide/Bis-Acrylamide	650 µL
1,5 M Tris-HCl (pH 8.8)	3.8 mL	0,5 M Tris-HCl (pH 6.8)	1.25 mL
10% SDS	100 µL	10% SDS	75 µL
10% APS	100 µL	10% APS	100 µL
TEMED	10 µL	TEMED	10 µL

Table C. 7. Buffers required for western blot.

10 X Running buffer	**Materials' amount (mass)**
Tris base	30.0 grams
Glycine	144.0 grams
10% SDS	10.0 grams
Dilute to 1X before use	100 mL 10X + 900 mL dH2O
10 X Transfer buffer	**Materials' amount (mass)**
Tris base	30.0 grams
Glycine	144.0 grams
Dilute to 1X and add methanol before use	100 mL 10X + 700 mL dH2O+ 200 mL methanol
10 X Tris buffered saline (TBS)	**Materials' amount (mass)**
Tris base	24.0 grams
NaCl	88.0 grams
Dilute to 1X before use	Dissolve in 1 L dH2O
1 X Tween-Tris buffered saline (T-TBS)	**Materials' amount (mL)**
1X TBS	500 mL
20% Tween	0.5 mL

APPENDIX D

CB1R AND MC3R'S CT VALUES

Table D. 1. CB1R's CT values

Mean Ct(CB1R)	CTRL1	CTRL2	OLA1	OLA2	OLA3
	14.68	19.23	19.27	19.61	19.43
	19.63	18.44	19.07	19.27	19.18
	16.57	18.53	19.6	19.33	19.25
	18.25	18.99	20.95	18.85	21.49
	19	17.94	19.77	19.25	20.79
	19.75	19.26	19.61	17.54	20.47
	17.49	18.03	20.15	19.26	21.2
	13.74	18.66	19.53	18.7	19.72
	17.9	22.04	18.67	18.71	21.8
	18.93	18.6	23.07	19.84	20.47
AVG	17.618	18.972	19.969	19.036	20.38

Table D. 2. MC3R's CT values

Mean CT (MC3R)	CTRL1	CTRL2	OLA1	OLA3
	26.56	18.95	22.81	25.4
	22.48	22.9	21.63	22.21
	22.23	21.7	22.67	21.42
	22.46	23.24	23.65	23.88
	22.09	20.94	22.38	22.565
	21.8	22.02	23.07	23.34
	20.205	20.78	22.55	23.105
	16.59	21.26	23.09	22.265
	20.515	24.27	21.43	24.05
	17.66	21.1	26.09	23.385
AVG	21.259	21.716	22.937	23.162

APPENDIX E

TOTAL PROTEIN CONCENTRATIONS OF ANIMAL GROUPS (µG/ML).

Table E. 1. CTRL1 Group

C1R1	C1R2	C1R3	C1R4
17.09	11.49	12.46	15.89
C2R1	C2R2	C2R3	C3R1
13.81	11.4	14.78	14.6

Table E. 2. CTRL2 Group

C4R1	C4R2	C4R3	C4R4	C5R1
14.21	10.62	14.54	14.47	10.39
C5R2	C5R3	C6R1	C6R3	
14.55	11.04	11.57	10.47	

Table E. 3. OLA1 Group

C7R1	C7R2	C7R3	C7R4	C8R1
19.64	15.58	15.67	12.7	20.15
C8R2	C8R3	C9R1	C9R2	C9R3
18.56	13.25	14.15	18.45	16.21

Table E. 4. OLA2 Group

C10R1	C10R2	C10R3	C10R4	C11R1
22.07	14.83	12.2	14.18	19.18
C11R2	C11R3	C12R1	C12R2	C12R3
11.79	21.85	18.41	12.87	14.07

Table E. 5. OLA3 Group

C13R1	C13R2	C13R3	C13R4	C14R1
26.16	21.01	19.67	22.34	22.21
C14R2	C14R3	C15R1	C15R2	C15R3
18.27	20.54	18.4	21.03	19.77

APPENDIX F

RELATIVE QUANTIFICATIONS OF PROTEINS AFTER WESTERN BLOT ANALYSIS.

Table F.1 listed the relative quantification of CTRL1 and OLA1 groups' representatives with C1R2 of CTRL1's group serving as the reference point. Gel 45 consisted of animals C1R2, C1R4, and C2R1 as CTRL1 group's representative. Meanwhile, C7R1, C7R2, C7R3, and C7R4 were from the OLA1 group.

Table F. 1. Gel 45 (CTRL1 and OLA1) relative protein quantification.

Animal Number and Group	Relative Quantifications	Relative Quantifications (Original)
C1R2 (CTRL1)	1,00 (Reference)	1,00
C1R4 (CTRL1)	1,04	0.290
C2R1 (CTRL1)	0,00	0.170
C7R1 (OLA1)	0,41	0.430
C7R2 (OLA1)	0,43	0.460
C7R3 (OLA1)	0,65	0.610
C7R4 (OLA1)	4,00	3.620

Table F.2 listed the relative quantification of CTRL1 and OLA1 groups' representatives with C2R2 of CTRL1's group serving as the reference point. Gel 46 consisted of animals C2R2, C2R3, and C3R1 as CTRL1 group's representative. Meanwhile, C8R1, C8R3, and C9R1 were from the OLA1 group.

Table F. 2. Gel 46 (CTRL1 and OLA1) relative protein quantification.

Animal Number and Group	Relative Quantifications	Relative Quantifications (Original)
C2R2 (CTRL1)	1,00 (Reference)	1.700
C2R3 (CTRL1)	3,02	3.470
C3R1 (CTRL1)	1,81	0.985
C8R1 (OLA1)	0,91	1.050
C8R3 (OLA1)	0,94	1.050
C9R1 (OLA1)	1,15	1.310

Table F.3 listed the relative quantification of CTRL2 and OLA2 groups' representatives with C4R2 of CTRL2's group serving as the reference point. Gel 47 consisted of animals C4R1, C4R2, C4R3, and C4R4 as CTRL2 group's representative. Meanwhile, C10R1, C10R2, C10R3, and C10R4 were from the OLA2 group.

Table F. 3. Gel 47 (CTRL2 and OLA2) relative protein quantification.

Animal Number and Group	Relative Quantifications	Relative Quantifications (Original)
C4R1 (CTRL2)	1,00 (Reference)	0.670
C4R2 (CTRL2)	0,68	0.790
C4R3 (CTRL2)	5,46	2.535
C4R4 (CTRL2)	4,81	2.400
C10R1 (OLA2)	2,85	2.710
C10R2 (OLA2)	1,36	2.270
C10R3 (OLA2)	6,57	6.690
C10R4 (OLA2)	2,59	2.680

Table F.4 listed the relative quantification of CTRL2 and OLA2 groups' representatives with C5R1 of CTRL2's group serving as the reference point. Gel 48 consisted of animals C4R1, C4R2, C4R3, and C4R4 as CTRL2 group's representative. Meanwhile, C10R1, C10R2, C10R3, and C10R4 were from the OLA2 group.

Table F. 4. Gel 48 (CTRL2 and OLA2) relative protein quantification.

Animal Number and Group	Relative Quantifications	Relative Quantifications (Original)
C5R1 (CTRL2)	1,00 (Reference)	3.750
C5R2 (CTRL2)	4,06	3.450
C5R3 (CTRL2)	4,58	4.260
C6R1 (CTRL2)	5,92	5.510
C11R1 (OLA2)	3,29	2.680
C11R2 (OLA2)	0,60	0.720
C11R3 (OLA2)	2,88	2.560
C12R1 (OLA2)	0,62	0.550

Table F.5 listed the relative quantification of OLA1, OLA2, and OLA3 groups' representatives with C9R2 of OLA1's group serving as the reference point. Gel 49 consisted of animals C9R2 for OLA1, C12R2 for OLA2, and C13R1, C13R2, C13R3, C13R4, and C14R1 as OLA3 group's representative.

Table F. 5. Gel 49 (OLA1, OLA2 and OLA3) relative protein quantification.

Animal Number and Group	Relative Quantifications	Relative Quantifications (Original)
C9R2 (OLA1)	1,00 (Reference)	1.300
C12R2 (OLA2)	0,43	0.440
C13R1 (OLA3)	1,53	1.41
C13R2 (OLA3)	1,32	1.27
C13R3 (OLA3)	0,80	0.85
C13R4 (OLA3)	0,42	0.52
C14R1 (OLA3)	0,52	0.75

Table F.6 listed the relative quantification of OLA1, OLA2, and OLA3 groups' representatives with C9R2 of OLA1's group serving as the reference point. Gel 49 consisted of animals C9R3 for OLA1, C12R3 for OLA2, and C13R1, C13R2, C13R3, C13R4, and C14R1 as OLA3 group's representative.

Table F. 6. Gel 50 (OLA1, OLA2 and OLA3) relative protein quantification.

Animal Number and Group	Relative Quantifications	Relative Quantifications (Original)
C9R3 (OLA1)	1,00 (Reference)	1.420
C12R3 (OLA2)	3,52	3.090
C14R2 (OLA3)	6,91	6.04
C14R3 (OLA3	3,52	4.22
C15R1 (OLA3)	5,80	4.87
C15R2 (OLA3)	6,91	5.56
C15R3 (OLA3)	1,65	1.61

APPENDIX G

ORIGINAL GEL PICTURES.

Gel 45 (CTRL1 and OLA1)

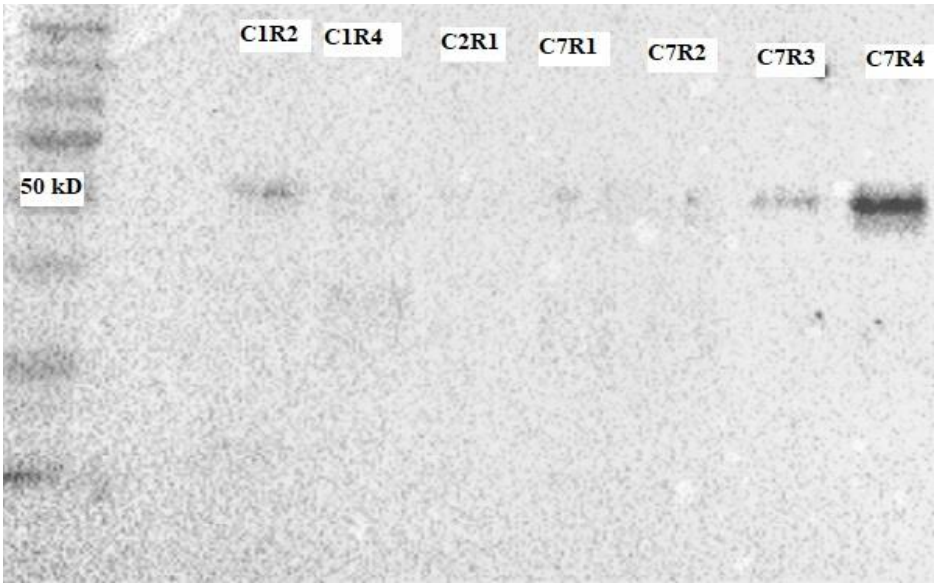

Figure G. 1. Western blot analysis of CTRL1 and OLA1 groups representatives of gel 45

Gel 46 (CTRL1 and OLA1)

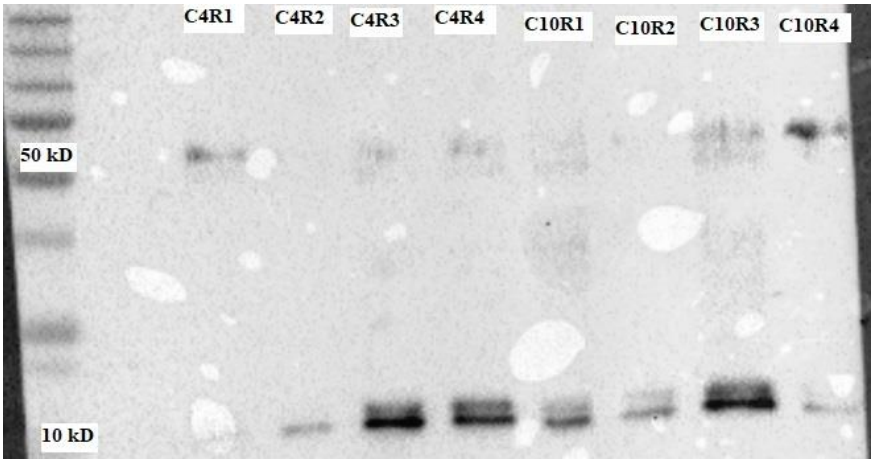

Figure G. 2. Western blot analysis of CTRL1 and OLA1 groups' representatives of gel 46.

Gel 47 (CTRL2 and OLA2)

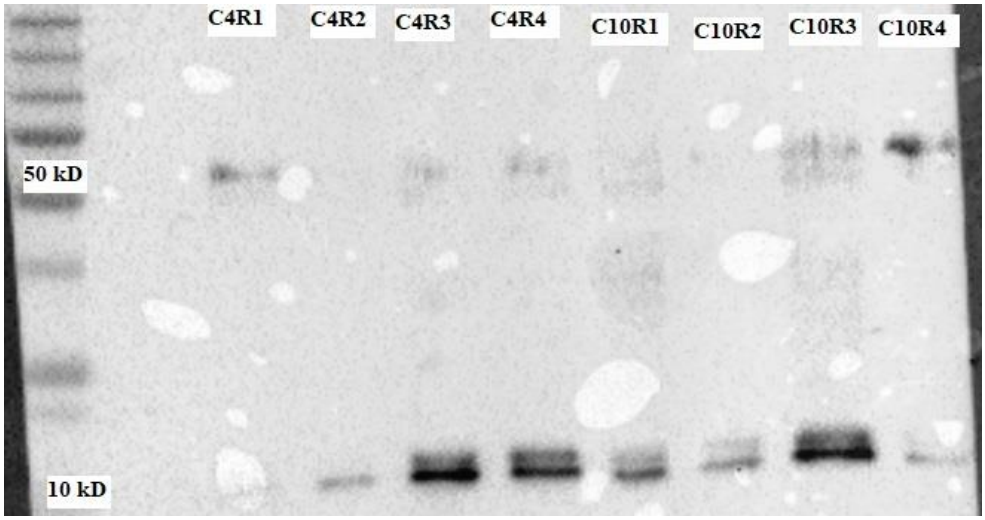

Figure G. 3. Western blot analysis of CTRL2 and OLA2 groups' representatives of gel 47.

Gel 48 (CTRL2 and OLA2)

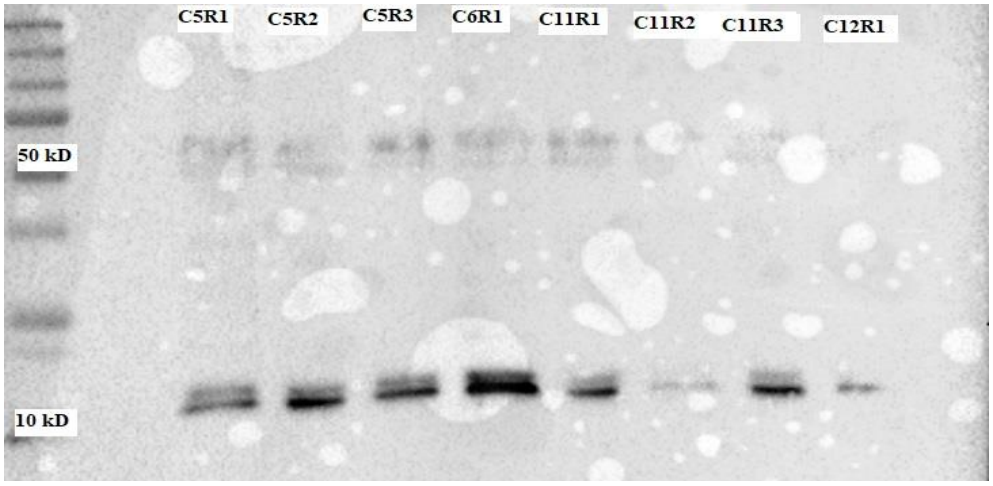

Figure G. 4. Western blot analysis of CTRL2 and OLA2 groups' representatives of gel 48.

Gel 49 (OLA1, OLA2, and OLA3)

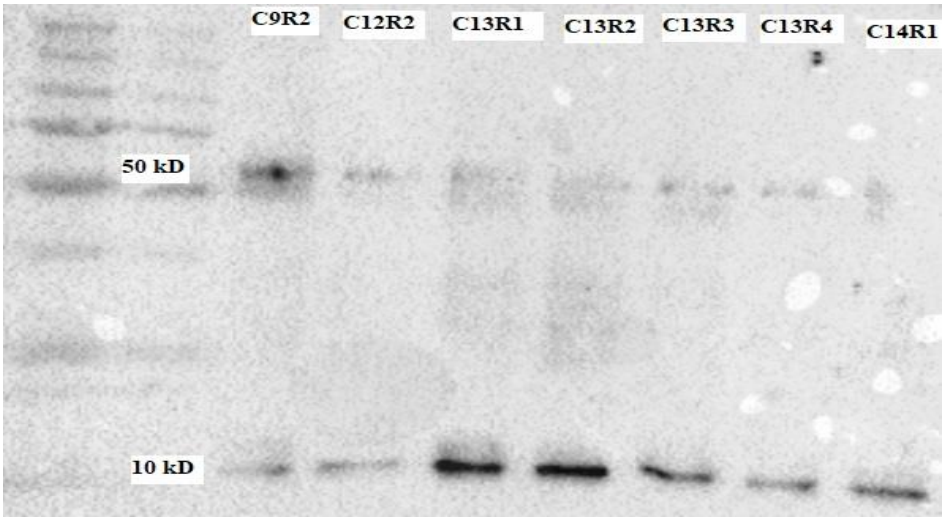

Figure G. 5. Western blot analysis of OLA1, OLA2, and OLA3 groups' representatives of gel 49.

Gel 50 (OLA1, OLA2, and OLA3)

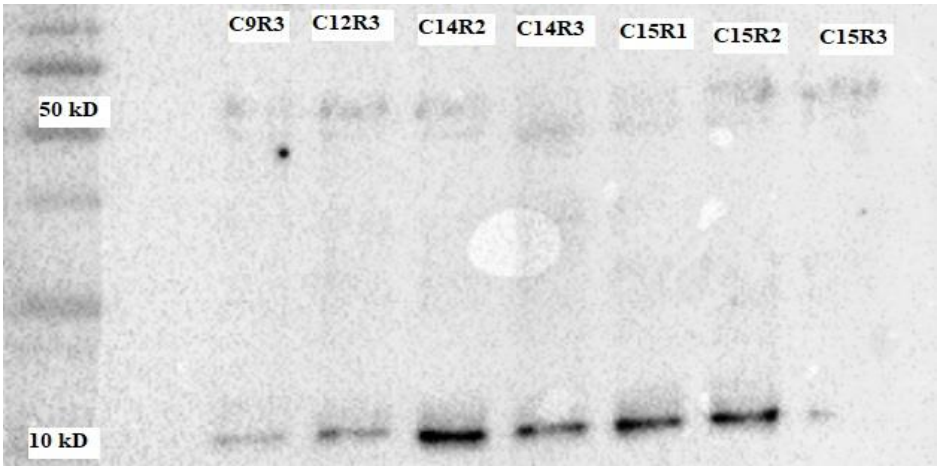

Figure G. 6. Western blot analysis of OLA1, OLA2, and OLA3 groups' representatives of gel 50.

APPENDIX H

RT-PCR GRAPHS.

CB1R graph

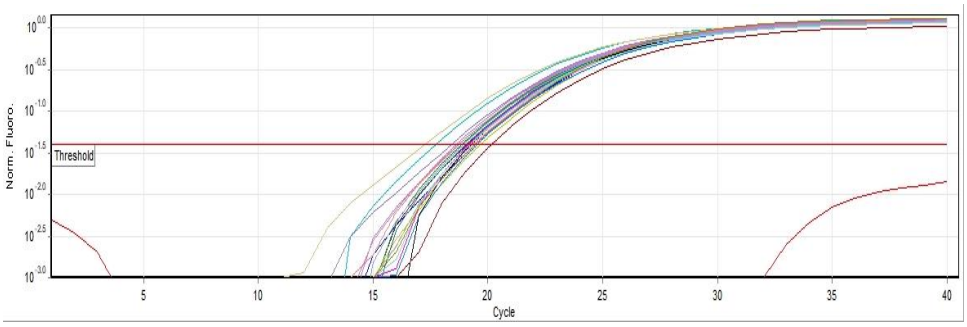

Figure H. 1. Amplification graph of OLA1 group for CB1R in RT-PCR.

MC3R graph

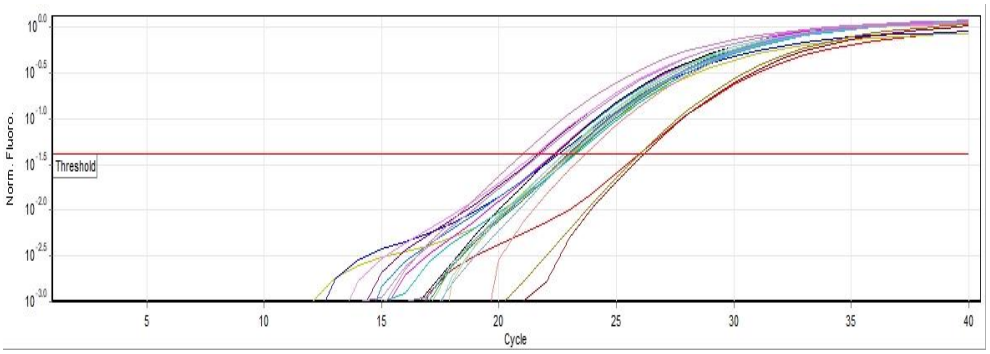

Figure H. 2. Amplification graph of OLA2 group for MC3R in RT-PCR.

APPENDIX I

NEUTRAL GEL RECIPE AND PICTURE.

Table I. 1. Separating gel (10%) and stacking gel (5%) of neutral polyacrylamide gel's compositions.

Components (Separating)	Volume
Water	19.3 mL
Lower Tris solution (1,5 M)	10 mL
40% Acrylamide	9.9 mL
50% Glycerol	240 µL
10% AmPSO4	240 µL
TEMED	20 µL
Components (Stacking)	Volume
Water	4.8 mL
Upper Tris solution (0,5 M)	2.0 mL
40% Acrylamide	1.0 mL
10% AmPSO4	80 µL
TEMED	8 µL

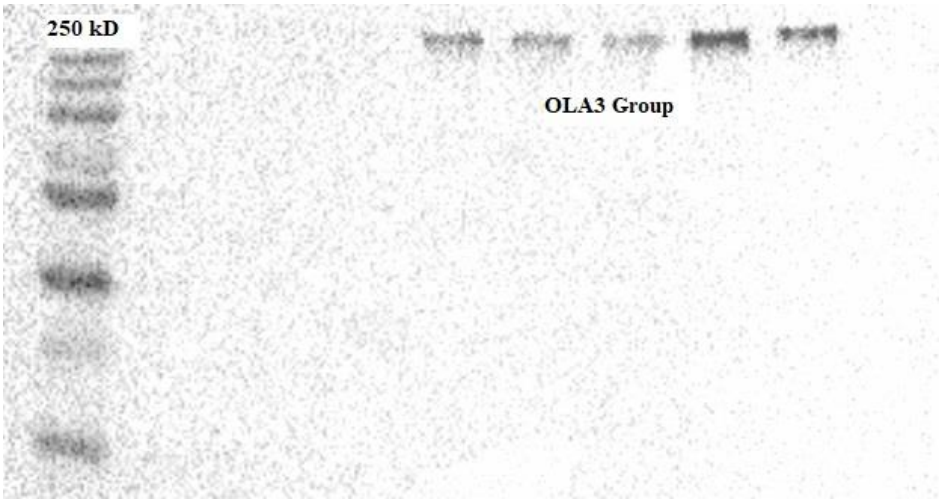

Figure I. 1. Neutral gel (with no application of SDS) of OLA3 group samples. The protein was unable to get into the wells, which might indicate dimerization of MC3R.